46. **Landau, N. R., M. Warton, and D. R. Littman.** 1988. The envelope glycoprotein of the human immunodeficiency virus binds to the immunoglobulin-like domain of CD4. Nature **334**:159–162.
47. **Lores, P., V. Boucher, C. Mackay, M. Pla, H. Von Boehmer, J. Jami, F. Barre-Sinoussi, and J. C. Weill.** 1992. Expression of human CD4 in transgenic mice does not confer sensitivity to human immunodeficiency virus infection. AIDS Res. Hum. Retrovir. **8**:2063–2071.
48. **Lu, Y. L., P. Spearman, and L. Ratner. 1993.** Human immunodeficiency virus type 1 viral protein R localization in infected cells and virions. J. Virol. **67**:6542–6550.
49. **Maddon, P. J., A. G. Dalgleish, J. S. McDougal, P. R. Clapham, R. A. Weiss, and R. Axel.** 1986. The T4 gene encodes the AIDS virus receptor and is expressed in the immune system and the brain. Cell **47**:333–348.
50. **Maertens, G., P. Cherepanov, W. Pluymers, K. Busschots, E. De Clercq, Z. Debyser, and Y. Engelborghs.** 2003. LEDGF/p75 is essential for nuclear and chromosomal targeting of HIV-1 integrase in human cells. J. Biol. Chem. **278**:33528–33539.
51. **Mancebo, H. S., G. Lee, J. Flygare, J. Tomassini, P. Luu, Y. Zhu, J. Peng, C. Blau, D. Hazuda, D. Price, and O. Flores.** 1997. P-TEFb kinase is required for HIV Tat transcriptional activation in vivo and in vitro. Genes Dev. **11**:2633–2644.
52. **Mariani, R., B. A. Rasala, G. Rutter, K. Wiegers, S. M. Brandt, H. G. Krausslich, and N. R. Landau.** 2001. Mouse-human heterokaryons support efficient human immunodeficiency virus type 1 assembly. J. Virol. **75**:3141–3151.
53. **Mariani, R., G. Rutter, M. E. Harris, T. J. Hope, H. G. Krausslich, and N. R. Landau.** 2000. A block to human immunodeficiency virus type 1 assembly in murine cells. J. Virol. **74**:3859–3870.
54. **Masuda, T., V. Planelles, P. Krogstad, and I. S. Chen.** 1995. Genetic analysis of human immunodeficiency virus type 1 integrase and the U3 att site: unusual phenotype of mutants in the zinc finger-like domain. J. Virol. **69**: 6687–6696.
55. **Miller, D. G., and A. D. Miller.** 1994. A family of retroviruses that utilize related phosphate transporters for cell entry. J. Virol. **68**:8270–8276.
56. **Morikawa, Y., S. Hinata, H. Tomoda, T. Goto, M. Nakai, C. Aizawa, H. Tanaka, and S. Omura. 1996.** Complete inhibition of human immunodeficiency virus Gag myristoylation is necessary for inhibition of particle budding. J. Biol. Chem. **271**:2868–2873.
57. **Neil, S., F. Martin, Y. Ikeda, and M. Collins.** 2001. Postentry restriction to human immunodeficiency virus-based vector transduction in human monocytes. J. Virol. **75**:5448–5456.
58. **Newstein, M., E. J. Stanbridge, G. Casey, and P. R. Shank.** 1990. Human chromosome 12 encodes a species-specific factor which increases human immunodeficiency virus type 1 tat-mediated trans activation in rodent cells. J. Virol. **64**:4565–4567.
59. **Nisole, S., and A. Saib.** 2004. Early steps of retrovirus replicative cycle. Retrovirology **1**:9.
60. **Nisole, S., J. P. Stoye, and A. Saib.** 2005. TRIM family proteins: retroviral restriction and antiviral defence. Nat. Rev. Microbiol. **3**:799–808.
61. **Nomura, H., B. W. Nielsen, and K. Matsushima.** 1993. Molecular cloning of cDNAs encoding a LD78 receptor and putative leukocyte chemotactic peptide receptors. Int. Immunol. **5**:1239–1249.
62. **Ory, D. S., B. A. Neugeboren, and R. C. Mulligan.** 1996. A stable human-derived packaging cell line for production of high titer retrovirus/vesicular stomatitis virus G pseudotypes. Proc. Natl. Acad. Sci. USA **93**:11400–11406.
63. **Petit, C., O. Schwartz, and F. Mammano.** 2000. The karyophilic properties of human immunodeficiency virus type 1 integrase are not required for nuclear import of proviral DNA. J. Virol. **74**:7119–7126.
64. **Piller, S. C., L. Caly, and D. A. Jans.** 2003. Nuclear import of the pre-integration complex (PIC): the Achilles heel of HIV? Curr. Drug Targets **4**:409–429.
65. **Planelles, V., A. Haislip, E. S. Withers-Ward, S. A. Stewart, Y. Xie, N. P. Shah, and I. S. Chen.** 1995. A new reporter system for detection of retroviral infection. Gene Ther. **2**:369–376.
66. **Pluymers, W., P. Cherepanov, D. Schols, E. De Clercq, and Z. Debyser.** 1999. Nuclear localization of human immunodeficiency virus type 1 integrase expressed as a fusion protein with green fluorescent protein. Virology **258**:327–332.
67. **Pollard, V. W., and M. H. Malim.** 1998. The HIV-1 Rev protein. Annu. Rev. Microbiol. **52**:491–532.
68. **Popov, S., M. Rexach, G. Zybarth, N. Reiling, M. A. Lee, L. Ratner, C. M. Lane, M. S. Moore, G. Blobel, and M. Bukrinsky.** 1998. Viral protein R regulates nuclear import of the HIV-1 pre-integration complex. EMBO J. **17**:909–917.
69. **Sakai, H., R. Shibata, J. Sakuragi, S. Sakuragi, M. Kawamura, and A. Adachi. 1993.** Cell-dependent requirement of human immunodeficiency virus type 1 Vif protein for maturation of virus particles. J. Virol. **67**:1663–1666.
70. **Sawada, S., K. Gowrishankar, R. Kitamura, M. Suzuki, G. Suzuki, S. Tahara, and A. Koito.** 1998. Disturbed CD4+ T cell homeostasis and in vitro HIV-1 susceptibility in transgenic mice expressing T cell line-tropic HIV-1 receptors. J. Exp. Med. **187**:1439–1449.
71. **Sherman, M. P., and W. C. Greene.** 2002. Slipping through the door: HIV entry into the nucleus. Microbes Infect. **4**:67–73.
72. **Stremlau, M., C. M. Owens, M. J. Perron, M. Kiessling, P. Autissier, and J. Sodroski.** 2004. The cytoplasmic body component TRIM5alpha restricts HIV-1 infection in Old World monkeys. Nature **427**:848–853.
73. **Suzuki, Y., N. Misawa, C. Sato, H. Ebina, T. Masuda, N. Yamamoto, and Y. Koyanagi. 2003.** Quantitative analysis of human immunodeficiency virus type 1 DNA dynamics by real-time PCR: integration efficiency in stimulated and unstimulated peripheral blood mononuclear cells. Virus Genes **27**:177–188.
74. **Tanaka, J., H. Ozaki, J. Yasuda, R. Horai, Y. Tagawa, M. Asano, S. Saijo, M. Imai, K. Sekikawa, M. Kopf, and Y. Iwakura.** 2000. Lipopolysaccharide-induced HIV-1 expression in transgenic mice is mediated by tumor necrosis factor-alpha and interleukin-1, but not by interferon-gamma nor interleukin-6. AIDS **14**:1299–1307.
75. **Tsuruo, T., T. Yamori, K. Naganuma, S. Tsukagoshi, and Y. Sakurai.** 1983. Characterization of metastatic clones derived from a metastatic variant of mouse colon adenocarcinoma 26. Cancer Res. **43**:5437–5442.
76. **Tsurutani, N., M. Kubo, Y. Maeda, T. Ohashi, N. Yamamoto, M. Kannagi, and T. Masuda. 2000.** Identification of critical amino acid residues in human immunodeficiency virus type 1 IN required for efficient proviral DNA formation at steps prior to integration in dividing and nondividing cells. J. Virol. **74**:4795–4806.
77. **van Maanen, M., and R. E. Sutton.** 2003. Rodent models for HIV-1 infection and disease. Curr. HIV Res. **1**:121–130.
78. **Wei, P., M. E. Garber, S. M. Fang, W. H. Fischer, and K. A. Jones.** 1998. A novel CDK9-associated C-type cyclin interacts directly with HIV-1 Tat and mediates its high-affinity, loop-specific binding to TAR RNA. Cell **92**:451–462.
79. **Yang, W. K., J. O. Kiggans, D. M. Yang, C. Y. Ou, R. W. Tennant, A. Brown, and R. H. Bassin.** 1980. Synthesis and circularization of N- and B-tropic retroviral DNA Fv-1 permissive and restrictive mouse cells. Proc. Natl. Acad. Sci. USA **77**:2994–2998.
80. **Yasuda, J., T. Miyao, M. Kamata, Y. Aida, and Y. Iwakura.** 2001. T cell apoptosis causes peripheral T cell depletion in mice transgenic for the HIV-1 vpr gene. Virology **285**:181–192.
81. **Zack, J. A., S. J. Arrigo, S. R. Weitsman, A. S. Go, A. Haislip, and I. S. Chen.** 1990. HIV-1 entry into quiescent primary lymphocytes: molecular analysis reveals a labile, latent viral structure. Cell **61**:213–222.
82. **Zennou, V., C. Petit, D. Guetard, U. Nerhbass, L. Montagnier, and P. Charneau.** 2000. HIV-1 genome nuclear import is mediated by a central DNA flap. Cell **101**:173–185.
83. **Zheng, Y. H., H. F. Yu, and B. M. Peterlin.** 2003. Human p32 protein relieves a post-transcriptional block to HIV replication in murine cells. Nat. Cell Biol. **5**:611–618.

Journal of General Virology (2007), 88, 3139–3144 DOI 10.1099/vir.0.83202-0

Short Communication

Inhibitory role of CXCR4 glycan in CD4-independent X4-tropic human immunodeficiency virus type 1 infection and its abrogation in CD4-dependent infection

Yoshinao Kubo,[1] Masaru Yokoyama,[1,2] Hiroaki Yoshii,[1] Chiho Mitani,[1] Chika Tominaga,[1] Yuetsu Tanaka,[3] Hironori Sato[1,2] and Naoki Yamamoto[1,4,5]

Correspondence
Yoshinao Kubo
yoshinao@net.nagasaki-u.ac.jp

[1]Department of AIDS Research, Institute of Tropical Medicine, Nagasaki University, Nagasaki, Japan

[2]Laboratory of Viral Genomics, Center for Pathogen Genomics, National Institute of Infectious Diseases, Tokyo, Japan

[3]Department of Immunology, Graduate School and Faculty of Medicine, University of the Ryukyus, Okinawa, Japan

[4]AIDS Research Center, National Institute of Infectious Diseases, Tokyo, Japan

[5]Department of Molecular Virology, Tokyo Medical and Dental University, Tokyo, Japan

CXCR4 functions as an infection receptor of X4 human immunodeficiency virus type 1 (HIV-1). CXCR4 is glycosylated at the N-terminal extracellular region, which is important for viral envelope (Env) protein binding. We compared the effects of CXCR4 glycan on the CD4-dependent and -independent infections in human cells by X4 viruses. We found that transduction mediated by Env proteins of CD4-independent HIV-1 strains increased up to 5.5-fold in cells expressing unglycosylated CXCR4, suggesting that the CXCR4 glycan inhibits CD4-independent X4 virus infection. Co-expression of CD4 on the target cell surface or pre-incubation of virus particles with soluble CD4 abrogates the glycan-mediated inhibition of X4 virus infection, suggesting that interaction of Env protein with CD4 counteracts the inhibition. These findings indicate that it will be advantageous for X4 HIV-1 to remain CD4-dependent. A structural model that explains the glycan-mediated inhibition is discussed.

Received 1 June 2007
Accepted 18 July 2007

Infection by the X4-tropic human immunodeficiency virus type 1 (HIV-1) requires interaction of two cellular surface proteins, CD4 and CXCR4 (Berger *et al.*, 1998; Dimitrov, 1997). CXCR4 is a multi-membrane-spanning protein that possesses an N-glycosylation site in the N-terminal extracellular region (Chabot *et al.*, 2000). Since the glycosylation site locates near the amino acid residues important for HIV-1 entry (Brelot *et al.*, 2000; Chabot & Broder, 2000; Chabot *et al.*, 1999; Picard *et al.*, 1997), the glycan may inhibit X4 virus infection. Consistently, previous studies using mink or canine cells have indicated that the glycan inhibits infections of HIV-1 and HIV-2 X4 viruses (Potempa *et al.*, 1997; Wang *et al.*, 2004). However, it is not known whether the glycan has the same effect in human cells, in which glycan modification or other cellular cofactors necessary for infection might be different from those in non-human cells. Furthermore, studies using human cells failed to observe such inhibitory effects (Brelot *et al.*, 2000; Chabot *et al.*, 2000; Picard *et al.*, 1997; Thordsen *et al.*, 2002). Thus, despite extensive studies, the role of the CXCR4 glycan in X4 virus infection remained to be determined.

As is the case for HIV-1, most simple retroviruses use N-glycosylated multi-membrane-spanning proteins as their receptors (Overbaugh *et al.*, 2001; Sommerfelt, 1999). In contrast to the HIV-1 studies, however, all the studies reproducibly indicated that the N-glycan on the receptors can efficiently suppress simple retrovirus infection (Kubo *et al.*, 2002; Marin *et al.*, 2003; Tailor *et al.*, 2000; Wilson & Eiden, 1991). Entry mechanisms of the simple retroviruses and HIV-1 are similar in that they use multi-membrane-spanning proteins, whereas they differ in that the simple retroviruses need only a single type of receptor. Therefore, we hypothesized that the initial binding of gp120 to CD4 might counteract the glycan-mediated block of X4 virus infection.

Supplementary material is available with the online version of this paper.

To examine this hypothesis, we established human NP2 and U87 cell lines (Soda *et al.*, 1999) that express C-terminally HA-tagged wild-type (wt) CXCR4 or N11A mediated by a murine leukaemia virus vector as reported previously (Kubo *et al.*, 2003). N11A is a CXCR4 mutant lacking the N-glycosylation site by substitution of the asparagine residue by an alanine (Fig. 1a). Western immunoblot analysis using the anti-HA monoclonal antibody showed that N11A migrated faster than wt CXCR4, consistent with the loss of the N-glycan by mutation (Supplementary Figure S1, available with the online version of this paper).

We examined if the lack of the glycan on CXCR4 could affect transduction titres of an HIV-1 vector (Naldini *et al.*, 1996) having CD4-independent mNDK (Dumonceaux *et al.*, 1998) or 8X (Hoffman *et al.*, 1999) HIV-1 gp120. The HIV-1 vector contains the *lacZ* gene as a marker (Chang *et al.*, 1999; Iwakuma *et al.*, 1999), and transduction titre was estimated by counting blue cells after X-Gal staining of the inoculated cells as reported previously (Kubo *et al.*, 2004). Infection of the NP2 and U87 cells expressing N11A resulted in a moderate but statistically significant increase in the mNDK transduction titres; titres in N11A-expressing cells were about 1.5 and 2.5-fold higher than those in wt-expressing cells (Fig. 1b). Levels of enhancement were greater with 8X vector; titres in N11A-expressing cells were about 2.0 and 5.5-fold higher than those in wt-expressing cells. In contrast, the lack of glycan did not cause significant changes in titres of the VSV-G-pseudotyped vector (Chang *et al.*, 1999).

We analysed levels of cell-surface expression of wt and N11A CXCR4 in NP2 and U87 cells by FACS with an anti-CXCR4 antibody (A80) that recognizes the third extracellular loop of CXCR4 (Tanaka *et al.*, 2001). Fluorescence intensities of N11A-expressing NP2 and U87 cells were about 2 to 10-fold lower than those of wt-expressing cells (Fig. 1c). If wt and N11A were expressed at the same level, N11A could be 15 to 25 times more susceptible to CD4-independent infection than wt in NP2 cells. Similarly, N11A could be 4 to 11 times more susceptible than wt in U87 cells. This indicates that the CXCR4 glycan significantly inhibits CD4-independent infection. However, treatment of wt CXCR4-expressing cells with tunicamycin, an N-glycosylation inhibitor, had severe cytotoxicity, especially in U87 cells, and did not increase 8X vector transduction titre.

We examined whether the CXCR4 glycan could influence X4 virus infection upon CD4-mediated infection. For this purpose, we established NP2 and U87 cell lines that express both CD4 and CXCR4. As was seen with the CD4-negative cell lines, the size of N11A was smaller than that of wt (Supplementary Figure S2, available with the online version of this paper). Similarly, fluorescence intensities of N11A-expressing NP2 and U87 cells detected by FACS analysis were about 2 and 10-fold lower than those of wt-expressing cells in CD4-positive cells, respectively (Fig. 2a and b).

We next measured the effect of CD4 expression on transduction efficiency of various Env-pseudotyped vectors. Transduction titres of the mNDK and 8X vectors in NP2 cells co-expressing CXCR4 and CD4 were about 100-fold higher than in cells expressing CXCR4 alone (Supplementary Figure S3, available with the online version of this paper), suggesting that constitutive exposure of the coreceptor-binding site in these CD4-independent gp120 is partial and that CD4-induced conformational changes result in the full exposure.

We examined whether the CXCR4 glycan could influence X4 virus infection upon CD4-mediated infection. The

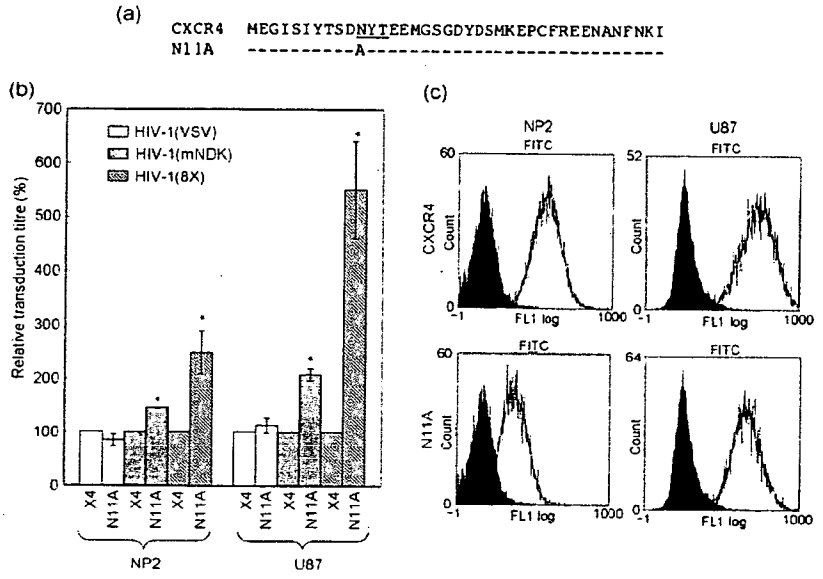

Fig. 1. Role of CXCR4 glycan in CD4-independent infection of X4 viruses. (a) Amino acid sequences of the N-terminal extracellular regions of wt CXCR4 and the N11A mutant. Hyphens indicate residues identical to wt CXCR4. The glycosylation site is underlined. The Asn residue was changed to Ala in the N11A mutant. (b) Relative transduction titres of the vectors in human cell lines expressing wt and N11A CXCR4. Relative titres to the titre in cells expressing wt CXCR4 (X4) are indicated. This experiment was repeated three times. Asterisks indicate statistical significance determined by Student's *t*-test, $P<0.05$. (c) Cell-surface expression was analysed with a flow cytometer and the anti-CXCR4 antibody (A80). The black area indicates control cells stained with the A80 antibody. The white area indicates wt CXCR4- and N11A mutant-expressing cells stained with the A80 antibody.

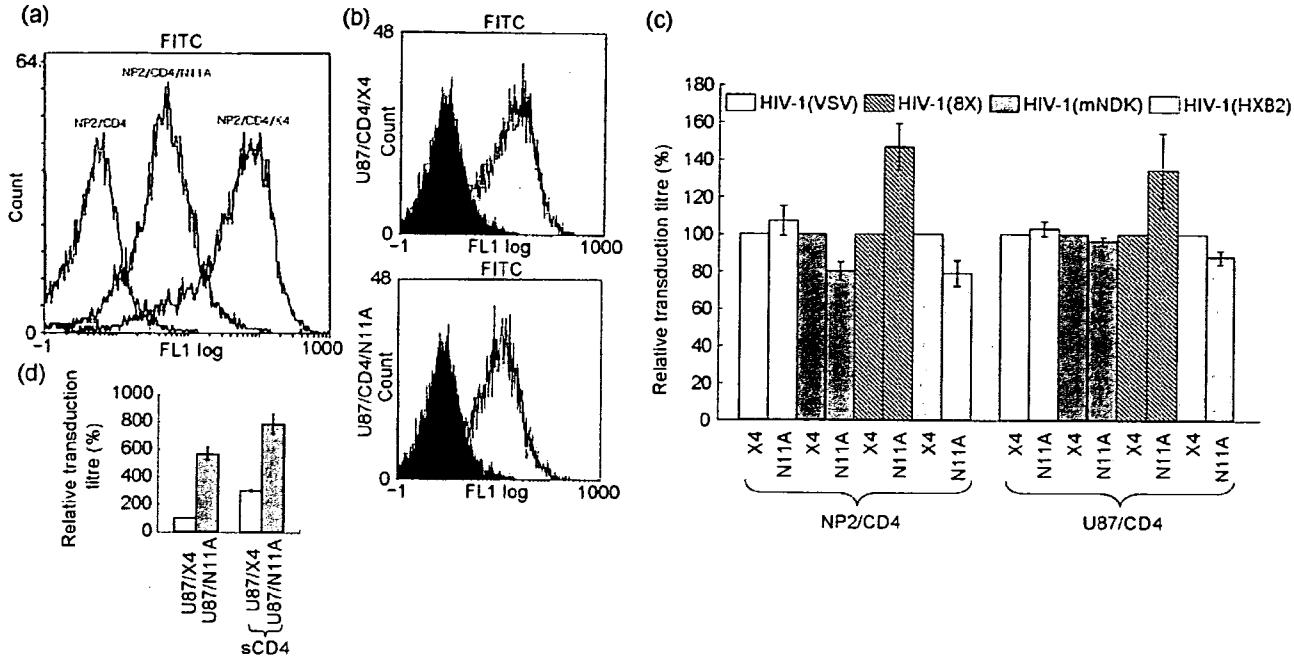

Fig. 2. CD4 counteracts CXCR4 glycan-mediated inhibition of X4 virus infection. (a, b) Cell-surface expression of wt CXCR4 and N11A mutant in NP2/CD4 (a) or U87/CD4 (b) cells was analysed with a flow cytometer and the anti-CXCR4 antibody A80. Black area indicates the control cells stained with A80. White area indicates wt CXCR4- and N11A mutant-expressing cells stained with A80. (c) Relative transduction titres of the vectors in human cells co-expressing CD4 and CXCR4. Relative titres to the titre in cells expressing CD4 and wt CXCR4 (X4) are indicated. Asterisks indicate statistical significance determined by Student's *t*-test, $P<0.05$. (d) Relative transduction titres of the 8X vector in the absence or presence of sCD4 (20 μg ml^{-1}). Relative titres to the titre in U87/X4 cells in the absence of sCD4 are indicated. These experiments were repeated three times.

vector solutions were diluted to obtain transduction titres similar to those of CD4-independent vectors in CD4-negative cells (about 5×10^2 infected cells per ml). Fig. 2(c) shows the relative transduction titres of the various Env-pseudotyped vectors in NP2 and U87 cells co-expressing CD4 and CXCR4. In contrast to the results with cells expressing N11A alone (Fig. 1), we could not detect a statistically significant increase in transduction titre of the vectors carrying the mNDK and the CD4-dependent HXB2 Env proteins in N11A-expressing cells. Similarly, removal of the CXCR4 glycan induced only a moderate increase in transduction titres of the 8X vector. These results showed that the mNDK, 8X and HXB2 viruses infected cells expressing wt CXCR4 as efficiently as cells expressing N11A when the target cells co-expressed CD4. These results suggest that the interaction of gp120 with CD4 counteracts the glycan-mediated inhibition.

To confirm this conclusion, we examined if preincubation of 8X vector particles with soluble CD4 (sCD4) could affect the glycan-mediated inhibition. The preincubation of sCD4 (20 μg ml^{-1}) enhanced transduction efficiency of the 8X vector approximately 3-fold in U87 cells expressing wt CXCR4 (Fig. 2d), as reported previously (Schenten *et al.*, 1999). In the absence of sCD4, the transduction titre in cells expressing N11A was about 5.5-fold higher than in cells expressing wt, but in the presence of sCD4, this difference was only 2.5-fold. This result indicates that sCD4 partially cancels the glycan-mediated inhibition of 8X virus infection, supporting the contention that CD4-gp120 interaction counteracts the glycan-mediated inhibition. The sCD4 treatment had lower efficiency to enhance the 8X vector infectivity and to counteract the glycan-mediated inhibition than the surface expression of CD4 on target cells. This may result from the dissociation of Env proteins from virus particles that is induced by the sCD4 treatment (Moore *et al.*, 1990; Hart *et al.*, 1991).

To help understand the molecular mechanisms by which the CXCR4 glycan affects the vector infectivity, we have built a three-dimensional (3D) model of CXCR4 with the carbohydrate moiety at the N terminus (Ponder & Case, 2003) (Fig. 3a). The crystal structure of the bovine rhodopsin [PDB code: 1F88 at 2.80 Å (0.28 nm) resolution] (Palczewski *et al.*, 2000) was used as a template for the homology modelling of CXCR4. The high-mannose carbohydrate structure was used as the N-glycan, so that we could examine minimum effects of steric hindrance against ligand access.

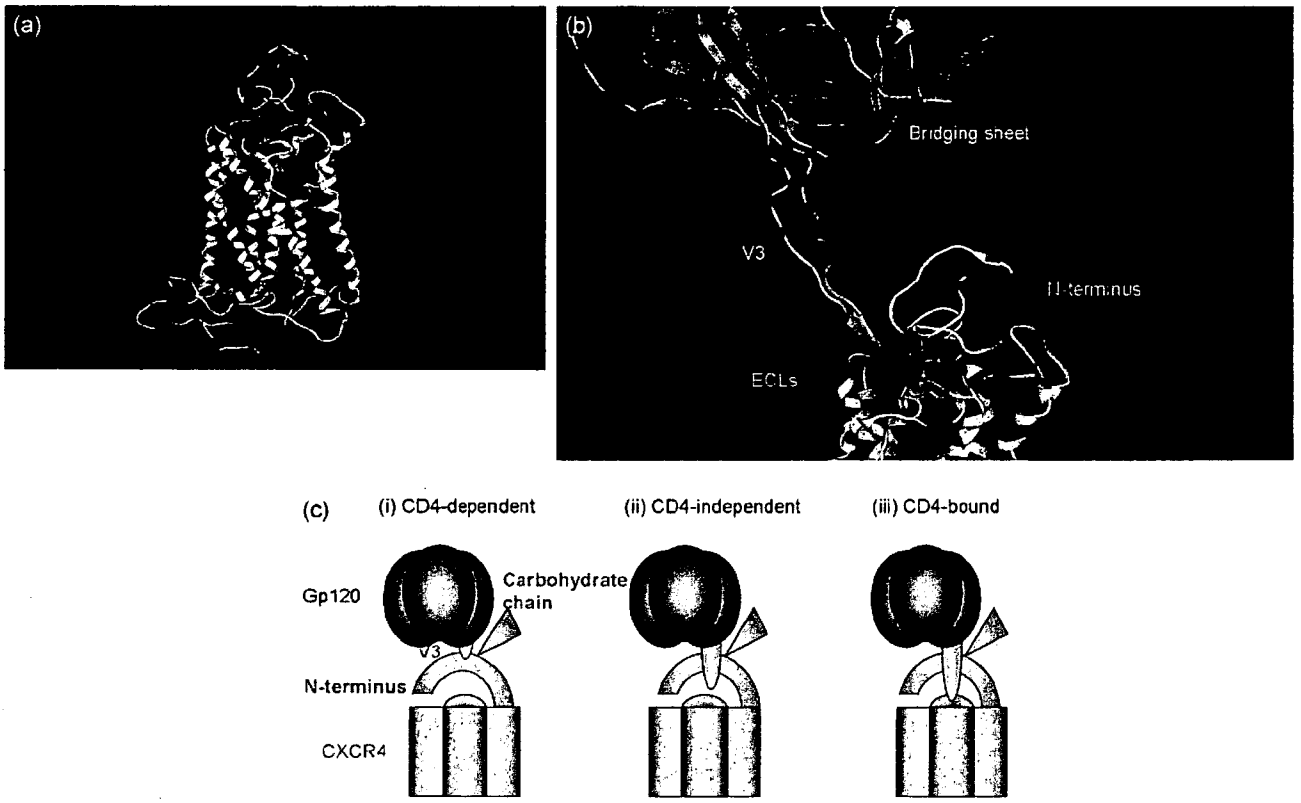

Fig. 3. Structural model of glycosylated CXCR4 and a schematic illustration of interactions between gp120 and CXCR4 during CD4-dependent and -independent infections. (a) The 3D structure of CXCR4 was constructed by homology modelling using the crystal structure of bovine rhodopsin. (b) Gp120 core with V3 (cyan, PDB code: 2B4C) was placed near the extracellular loops of the CXCR4 model (white). The purple residue indicates the glycosylated Asn. Red, blue and green residues indicate acidic, basic and uncharged polar amino acids, respectively. (c) Schematic illustration of a model of interactions between gp120 and CXCR4 during CD4-dependent and -independent infections. (i) Before CD4 binding, the V3 can rarely interact with CXCR4 due to low exposure of the CXCR4-binding moiety. (ii) After conformational change of gp120 upon binding to CD4, the V3 tip can reach the binding sites on CXCR4 due to the high level of V3 exposure. (iii) In case of the CD4-independent infection, V3 exposure is constitutive but partial, which increases sensitivity to the steric hindrance of the glycan.

Ramachandran plot, χ plot and energy minimization with AMBER-99 force field showed that the 3D model was physically and thermodynamically favoured and that it also preserves the physico-chemical features of the CXCR4 structure that were reported previously (Huang *et al.*, 2003). These features include high levels of negative electrostatic potential along the top of the extracellular surface region of CXCR4 (Fig. 3a, red residues). The negative amino acids are located on the N-terminal end and extracellular loops (ECL) 1, 2 and 3, and some of them are indicated to play important roles in binding to gp120 (Brelot *et al.*, 1997, 2000; Chabot *et al.*, 1999; Doranz *et al.*, 1999; Kajumo *et al.*, 2000; Zhou *et al.*, 2001). The 3D model suggests that these residues can function as attracting force via Coulombic interactions in the gp120 binding. In addition, the model shows that the glycan at the N terminus protrudes over this negatively charged region, narrowing space for HIV-1 Env protein access.

We found that X4 virus infectivity increased 1.5 to 5.5-fold when the virus infected human cells expressing N11A. Such an increase can be achieved by two mechanisms. First, N11A might have induced a conformation for increased binding to gp120. However, this possibility is unlikely because *in silico* structural analysis of the unglycosylated CXCR4 was nearly identical to the glycosylated counterpart. Furthermore, it is difficult to explain our results of the CD4-co-expression experiments by this mechanism. Our CXCR4 structural model supports the steric hindrance mechanism by predicting that the glycan will narrow the entry space of gp120 V3 (Fig. 3b). Unfortunately, a binding assay (Kinomoto *et al.*, 2005) did not show higher levels of 8X vector binding to N11A-expressing cells compared with wt-expressing cells (Supplementary Figure S4, available with the online version of this paper), due to the lower sensitivity of the binding assay than the vector transduction assay.

Our findings have implications for the importance of the CD4-dependent infection. CD4-independent variants are attenuated variants that are sensitive to antibody neutralization and that exist in nature only as a minor variant. CD4-dependency seems to have evolved to protect from neutralization antibodies (Bhattacharya *et al.*, 2003; Edwards *et al.*, 2001; Hoffman *et al.*, 1999; Kolchinsky *et al.*, 2001; Puffer *et al.*, 2002; Thomas *et al.*, 2003). Our data suggest that the CD4-dependent infection confers additional selective advantage other than a better defence capability. CD4-dependent viral infection was about 100-fold more efficient than CD4-independent infection. In addition, the glycan-mediated block of infection was counteracted by CD4-dependent infection. These data indicate that the CD4-independent X4 virus gains much better infectivity of human cells by CD4-mediated entry. Thus, CD4-dependent viruses dominate in nature possibly because they have a better defence capability against host immune restriction and better infectivity.

On the basis of our data and those of others, we suggest a model for the interactions between gp120 and CXCR4 upon CD4-mediated and -independent infections. Before the virus binds to CD4, the V3 loop in gp120 is less exposed (Zhu *et al.*, 2006) [Fig. 3c(i)]. Upon viral binding to CD4, massive conformational changes in gp120 induce full exposure of V3 (Huang *et al.*, 2005) [Fig. 3c(iii)] so that glycan-mediated inhibition is less efficient, leading to increase in viral infectivity, as seen in this and other studies (Brelot *et al.*, 2000; Chabot *et al.*, 2000; Picard *et al.*, 1997; Thordsen *et al.*, 2002). In the case of CD4-independent infection, however, V3 is constitutively but partially exposed (Edinger *et al.*, 1999; Edwards *et al.*, 2001; Hoffman *et al.*, 2000; Martin *et al.*, 1997), which increases sensitivity to the glycan effect [Fig. 3c(ii)]. This in turn decreases infectivity in cells expressing glycosylated CXCR4 (Potempa *et al.*, 1997; Wang *et al.*, 2004). Further biochemical studies including structure–function analysis of gp120 and receptors will help in our understanding of how the glycan on the infection receptor affect HIV infection.

Acknowledgements

We thank Dr D. Trono for the HIV-1 packaging construct (R8.91), Drs U. Hazan, R. Doms and Y. Yokomaku for the Env expression plasmids, Dr H. Hoshino for NP2 and U87 cells, and Dr K. Tokunaga for technical advice on the binding assay. The VSV-G expression plasmid and the LacZ-containing HIV-1 vector DNA were provided by Dr L. Chang through the AIDS Research and Reference Reagent Program, Division of AIDS, NIAID, NIH, USA. The sCD4 was also obtained from the above program. This work was supported by a Health Science Research Grant from the Ministry of Health, Labour and Welfare of Japan, and by the 21st century Centers of Excellence (COE) program.

References

Berger, E. A., Doms, R. W., Fenyo, E. M., Korber, B. T., Littman, D. R., Moore, J. P., Sattentau, Q. J., Schuitemaker, H., Sodroski, J. & Weiss, R. A. (1998). A new classification for HIV-1. *Nature* **391**, 240.

Bhattacharya, J., Peters, P. J. & Clapham, P. R. (2003). CD4-independent infection of HIV and SIV: implications for envelope conformation and cell tropism in vivo. *AIDS* **17** (*Suppl. 4*), S35–S43.

Brelot, A., Heveker, N., Pleskoff, O., Sol, N. & Alizon, M. (1997). Role of the first and third extracellular domains of CXCR-4 in human immunodeficiency virus coreceptor activity. *J Virol* **71**, 4744–4751.

Brelot, A., Heveker, N., Montes, M. & Alizon, M. (2000). Identification of residues of CXCR4 critical for human immunodeficiency virus coreceptor and chemokine receptor activities. *J Biol Chem* **275**, 23736–23744.

Chabot, D. J. & Broder, C. C. (2000). Substitutions in a homologous region of extracellular loop 2 of CXCR4 and CCR5 alter coreceptor activities for HIV-1 membrane fusion and virus entry. *J Biol Chem* **275**, 23774–23782.

Chabot, D. J., Zhang, P. F., Quinnan, G. V. & Broder, C. C. (1999). Mutagenesis of CXCR4 identifies important domains for human immunodeficiency virus type 1 X4 isolate envelope-mediated membrane fusion and virus entry and reveals cryptic coreceptor activity for R5 isolates. *J Virol* **73**, 6598–6609.

Chabot, D. J., Chen, H., Dimitrov, D. S. & Broder, C. C. (2000). N-linked glycosylation of CXCR4 masks coreceptor function for CCR5-dependent human immunodeficiency virus type 1 isolates. *J Virol* **74**, 4404–4413.

Chang, L. J., Urlacher, V., Iwakuma, T., Cui, Y. & Zucali, J. (1999). Efficacy and safety analyses of a recombinant human immunodeficiency virus type 1 derived vector system. *Gene Ther* **6**, 715–728.

Dimitrov, D. S. (1997). How do viruses enter cells? The HIV coreceptors teach us a lesson of complexity. *Cell* **91**, 721–730.

Doranz, B. J., Orsini, M. J., Turner, J. D., Hoffman, T. L., Berson, J. F., Hoxie, J. A., Peiper, S. C., Brass, L. F. & Doms, R. W. (1999). Identification of CXCR4 domains that support coreceptor and chemokine receptor functions. *J Virol* **73**, 2752–2761.

Dumonceaux, J., Nisole, S., Chanel, C., Quivet, L., Amara, A., Baleux, F., Briand, P. & Hazan, U. (1998). Spontaneous mutations in the env gene of the human immunodeficiency virus type 1 NDK isolate are associated with a CD4-independent entry phenotype. *J Virol* **72**, 512–519.

Edinger, A. L., Blanpain, C., Kunstman, K. J., Wolinsky, S. M., Parmentier, M. & Doms, R. W. (1999). Functional dissection of CCR5 coreceptor function through the use of CD4-independent simian immunodeficiency virus strains. *J Virol* **73**, 4062–4073.

Edwards, T. G., Hoffman, T. L., Baribaud, F., Wyss, S., LaBranche, C. C., Romano, J., Adkinson, J., Sharron, M., Hoxie, J. A. & Doms, R. W. (2001). Relationships between CD4 independence, neutralization sensitivity, and exposure of a CD4-induced epitope in a human immunodeficiency virus type 1 envelope protein. *J Virol* **75**, 5230–5239.

Hart, T. K., Kirsh, R., Ellens, H., Sweet, R. W., Lambert, D. M., Petteway, S. R., Jr, Leary, J. & Bugelski, P. J. (1991). Binding of soluble CD4 proteins to human immunodeficiency virus type 1 and infected cells induces release of envelope glycoprotein gp120. *Proc Natl Acad Sci U S A* **88**, 2189–2193.

Hoffman, T. L., LaBranche, C. C., Zhang, W., Canziani, G., Robinson, J., Chaiken, I., Hoxie, J. A. & Doms, R. W. (1999). Stable exposure of the coreceptor-binding site in a CD4-independent HIV-1 envelope protein. *Proc Natl Acad Sci U S A* **96**, 6359–6364.

Hoffman, T. L., Canziani, G., Jia, L., Rucker, J. & Doms, R. W. (2000). A biosensor assay for studying ligand-membrane receptor interactions: binding of antibodies and HIV-1 Env to chemokine receptors. *Proc Natl Acad Sci U S A* **97**, 11215–11220.

Huang, X., Shen, J., Cui, M., Shen, L., Luo, X., Ling, K., Pei, G., Jiang, H. & Chen, K. (2003). Molecular dynamics simulations on SDF-1alpha: binding with CXCR4 receptor. *Biophys J* **84**, 171–184.

Huang, C. C., Tang, M., Zhang, M. Y., Majeed, S., Montabana, E., Stanfield, R. L., Dimitrov, D. S., Korber, B., Sodroski, J. & other authors (2005). Structure of a V3-containing HIV-1 gp120 core. *Science* **310**, 1025–1028.

Iwakuma, T., Cui, Y. & Chang, L. J. (1999). Self-inactivating lentiviral vectors with U3 and U5 modifications. *Virology* **261**, 120–132.

Kajumo, F., Thompson, D. A., Guo, Y. & Dragic, T. (2000). Entry of R5X4 and X4 human immunodeficiency virus type 1 strains is mediated by negatively charged and tyrosine residues in the amino-terminal domain and the second extracellular loop of CXCR4. *Virology* **271**, 240–247.

Kinomoto, M., Yokoyama, M., Sato, H., Kojima, A., Kurata, T., Ikuta, K., Sata, T. & Tokunaga, K. (2005). Amino acid 36 in the human immunodeficiency virus type 1 gp41 ectodomain controls fusogenic activity: implications for the molecular mechanism of viral escape from a fusion inhibitor. *J Virol* **79**, 5996–6004.

Kolchinsky, P., Kiprilov, E. & Sodroski, J. (2001). Increased neutralization sensitivity of CD4-independent human immunodeficiency virus variants. *J Virol* **75**, 2041–2050.

Kubo, Y., Ono, T., Ogura, M., Ishimoto, A. & Amanuma, H. (2002). A glycosylation-defective variant of the ecotropic murine retrovirus receptor is expressed in rat XC cells. *Virology* **303**, 338–344.

Kubo, Y., Ishimoto, A. & Amanuma, H. (2003). N-Linked glycosylation is required for XC cell-specific syncytium formation by the R peptide-containing envelope protein of ecotropic murine leukemia viruses. *J Virol* **77**, 7510–7516.

Kubo, Y., Ishimoto, A., Ono, T., Yoshii, H., Tominaga, C., Mitani, C., Amanuma, H. & Yamamoto, N. (2004). Determinant for the inhibition of ecotropic murine leukemia virus infection by N-linked glycosylation of the rat receptor. *Virology* **330**, 82–91.

Marin, M., Lavillette, D., Kelly, S. M. & Kabat, D. (2003). N-linked glycosylation and sequence changes in a critical negative control region of the ASCT1 and ASCT2 neutral amino acid transporters determine their retroviral receptor functions. *J Virol* **77**, 2936–2945.

Martin, K. A., Wyatt, R., Farzan, M., Choe, H., Marcon, L., Desjardins, E., Robinson, J., Sodroski, J., Gerard, C. & Gerard, N. P. (1997). CD4-independent binding of SIV gp120 to rhesus CCR5. *Science* **278**, 1470–1473.

Moore, J. P., McKeating, J. A., Weiss, R. A. & Sattentau, Q. J. (1990). Dissociation of gp120 from HIV-1 virions induced by soluble CD4. *Science* **250**, 1139–1142.

Naldini, L., Blomer, U., Gallay, P., Ory, D., Mulligan, R., Gage, F. H., Verma, I. M. & Trono, D. (1996). In vivo gene delivery and stable transduction of nondividing cells by a lentiviral vector. *Science* **272**, 263–267.

Overbaugh, J., Miller, A. D. & Eiden, M. V. (2001). Receptors and entry cofactors for retroviruses include single and multiple transmembrane-spanning proteins as well as newly described glycophosphatidylinositol-anchored and secreted proteins. *Microbiol Mol Biol Rev* **65**, 371–389 (table of contents).

Palczewski, K., Kumasaka, T., Hori, T., Behnke, C. A., Motoshima, H., Fox, B. A., Le Trong, I., Teller, D. C., Okada, T. & other authors (2000). Crystal structure of rhodopsin: A G protein-coupled receptor. *Science* **289**, 739–745.

Picard, L., Wilkinson, D. A., McKnight, A., Gray, P. W., Hoxie, J. A., Clapham, P. R. & Weiss, R. A. (1997). Role of the amino-terminal extracellular domain of CXCR-4 in human immunodeficiency virus type 1 entry. *Virology* **231**, 105–111.

Ponder, J. W. & Case, D. A. (2003). Force fields for protein simulations. *Adv Protein Chem* **66**, 27–85.

Potempa, S., Picard, L., Reeves, J. D., Wilkinson, D., Weiss, R. A. & Talbot, S. J. (1997). CD4-independent infection by human immunodeficiency virus type 2 strain ROD/B: the role of the N-terminal domain of CXCR-4 in fusion and entry. *J Virol* **71**, 4419–4424.

Puffer, B. A., Pohlmann, S., Edinger, A. L., Carlin, D., Sanchez, M. D., Reitter, J., Watry, D. D., Fox, H. S., Desrosiers, R. C. & Doms, R. W. (2002). CD4 independence of simian immunodeficiency virus Envs is associated with macrophage tropism, neutralization sensitivity, and attenuated pathogenicity. *J Virol* **76**, 2595–2605.

Schenten, D., Marcon, L., Karlsson, G. B., Parolin, C., Kodama, T., Gerard, N. & Sodroski, J. (1999). Effects of soluble CD4 on simian immunodeficiency virus infection on CD4-positive and CD4-negative cells. *J Virol* **73**, 5373–5380.

Soda, Y., Shimizu, N., Jinno, A., Liu, H. Y., Kanbe, K., Kitamura, T. & Hoshino, H. (1999). Establishment of a new system for determination of coreceptor usages of HIV based on the human glioma NP-2 cell line. *Biochem Biophys Res Commun* **258**, 313–321.

Sommerfelt, M. A. (1999). Retrovirus receptors. *J Gen Virol* **80**, 3049–3064.

Tailor, C. S., Nouri, A. & Kabat, D. (2000). Cellular and species resistance to murine amphotropic, gibbon ape, and feline subgroup C leukemia viruses is strongly influenced by receptor expression levels and by receptor masking mechanisms. *J Virol* **74**, 9797–9801.

Tanaka, R., Yoshida, A., Murakami, T., Baba, E., Lichtenfeld, J., Omori, T., Kimura, T., Tsurutani, N., Fujii, N. & other authors (2001). Unique monoclonal antibody recognizing the third extracellular loop of CXCR4 induces lymphocyte agglutination and enhances human immunodeficiency virus type 1-mediated syncytium formation and productive infection. *J Virol* **75**, 11534–11543.

Thomas, E. R., Shotton, C., Weiss, R. A., Clapham, P. R. & McKnight, A. (2003). CD4-dependent and CD4-independent HIV-2: consequences for neutralization. *AIDS* **17**, 291–300.

Thordsen, I., Polzer, S. & Schreiber, M. (2002). Infection of cells expressing CXCR4 mutants lacking N-glycosylation at the N-terminal extracellular domain is enhanced for R5X4-dualtropic human immunodeficiency virus type-1. *BMC Infect Dis* **2**, 31.

Wang, J., Babcock, G. J., Choe, H., Farzan, M., Sodroski, J. & Gabuzda, D. (2004). N-linked glycosylation in the CXCR4 N-terminus inhibits binding to HIV-1 envelope glycoproteins. *Virology* **324**, 140–150.

Wilson, C. A. & Eiden, M. V. (1991). Viral and cellular factors governing hamster cell infection by murine and gibbon ape leukemia viruses. *J Virol* **65**, 5975–5982.

Zhou, N., Luo, Z., Luo, J., Liu, D., Hall, J. W., Pomerantz, R. J. & Huang, Z. (2001). Structural and functional characterization of human CXCR4 as a chemokine receptor and HIV-1 co-receptor by mutagenesis and molecular modeling studies. *J Biol Chem* **276**, 42826–42833.

Zhu, P., Liu, J., Bess, J., Jr, Chertova, E., Lifson, J. D., Grise, H., Ofek, G. A., Taylor, K. A. & Roux, K. H. (2006). Distribution and three-dimensional structure of AIDS virus envelope spikes. *Nature* **441**, 847–852.

Inhibiting lentiviral replication by HEXIM1, a cellular negative regulator of the CDK9/cyclin T complex

Saki Shimizu[a,b], Emiko Urano[a], Yuko Futahashi[a], Kosuke Miyauchi[a], Maya Isogai[a], Zene Matsuda[a], Kyoko Nohtomi[a], Toshinari Onogi[a], Yutaka Takebe[a], Naoki Yamamoto[a,b] and Jun Komano[a]

Objective: Tat-dependent transcriptional elongation is crucial for the replication of HIV-1 and depends on positive transcription elongation factor b complex (P-TEFb), composed of cyclin dependent kinase 9 (CDK9) and cyclin T. Hexamethylene bisacetamide-induced protein 1 (HEXIM1) inhibits P-TEFb in cooperation with 7SK RNA, but direct evidence that this inhibition limits the replication of HIV-1 has been lacking. In the present study we examined whether the expression of FLAG-tagged HEXIM1 (HEXIM1-f) affected lentiviral replication in human T cell lines.

Methods: HEXIM1-f was introduced to five human T cell lines, relevant host for HIV-1, by murine leukemia virus vector and cells expressing HEXIM1-f were collected by fluorescence activated cell sorter. The lentiviral replication kinetics in HEXIM1-f-expressing cells was compared with that in green fluorescent protein (GFP)-expressing cells.

Results: HIV-1 and simian immunodeficiency virus replicated less efficiently in HEXIM1-f-expressing cells than in GFP-expressing cells of the five T cell lines tested. The viral revertants were not immediately selected in culture. In contrast, the replication of vaccinia virus, adenovirus, and herpes simplex virus type 1 was not limited. The quantitative PCR analyses revealed that the early phase of viral life cycle was not blocked by HEXIM1. On the other hand, *Tat*-dependent transcription in HEXIM1-f-expressing cells was substantially repressed as compared with that in GFP-expressing cells.

Conclusion: These data indicate that HEXIM1 is a host factor that negatively regulates lentiviral replication specifically. Elucidating the regulatory mechanism of HEXIM1 might lead to ways to control lentiviral replication.

AIDS 2007, **21**:575–582

Keywords: CDK9, cyclin T, HEXIM1, lentivirus, *tat*

Introduction

Activation of transcription elongation requires the positive transcription elongation factor b complex (P-TEFb) composed of cyclin dependent kinase 9 (CDK9) and cyclin T1, T2, or K [1]. P-TEFb is essential for efficient transcriptional elongation from the promoter of human immunodeficiency virus type 1 (HIV-1), the long terminal repeat (LTR) (reviewed in [2,3]). The functional interaction between P-TEFb and the viral protein Tat has been well studied. Immediately after viral transcription starts at the LTR of the integrated proviral genome, the nascent viral transcript forms a three-dimensional structure called TAR. In the presence of P-TEFb, Tat binds to TAR. Through the Tat–TAR interaction, Tat activates P-TEFb and therefore assures the efficient

From the [a]AIDS Research Center, National Institute of Infectious Diseases, Tokyo, and the [b]Department of Molecular Virology, Tokyo Medical and Dental University, Tokyo, Japan.

Correspondence to Jun Komano, AIDS Research Center, National Institute of Infectious Diseases, 1-23-1 Toyama, Shinjuku, Tokyo 162-8640, Japan.

E-mail: ajkomano@nih.go.jp

Received: 9 July 2006; revised: 25 October 2006; accepted: 13 November 2006.

ISSN 0269-9370 © 2007 Lippincott Williams & Wilkins

completion of viral gene transcription and the propagation of HIV-1.

Recently, the regulatory mechanisms of P-TEFb function have been elucidated. In 2001, the interaction of P-TEFb with 7SK RNA was found to be necessary to inactivate the kinase activity of CDK9 within P-TEFb [4–6]. However, the binding of 7SK RNA alone is not sufficient to inactivate P-TEFb. More recently, Yik *et al.* demonstrated that the inactivation of P-TEFb requires hexamethylene bisacetamide-induced protein 1 (HEXIM1; synonyms CLP1, MAQ1, and HIS1) [7–9]. The inactivation of P-TEFb by the HEXIM1-7SK RNA complex appears to regulate the transcriptional elongation of cellular genes.

The HEXIM1-7SK RNA complex has been shown to physically compete with Tat for binding to P-TEFb [10]. In agreement with this finding, HEXIM1 was shown to inhibit Tat-dependent transcription from the HIV-1 LTR in transient transfection assays [8,11,12]. However, no data demonstrating that HEXIM1 is able to limit HIV-1 replication has been provided. Here we provide direct experimental evidence that the constitutive expression of HEXIM1 specifically limits lentiviral replication.

Methods

Plasmids

The FLAG-tagged HEXIM1 expression constructs were generated by reverse-transcription PCR using RNA isolated from CEM cells as templates. The primers used were 5′-CACCTCGAGCCACCATGGACTACAAAGACGATGACGACAAGGCCGAGCCATTCTTGTC-3′ and 5′-CAATTGCTAGTCTCCAAACTTGGAAAGCGGCGC-3′′ for amino terminus FLAG tagging, and 5′-CACCTCGAGCCACCATGGCCGAGCCATTCTTGTCAGAATATC-3′ and 5′-CAATTGCTAGTCGTCATCGTCTTTGTAGTCGTCTCCAAACTTGGAAAGCGGCGCTC-3′ for carboxy terminus FLAG tagging. The *Xho*I-*Mfe*I fragments of the PCR products were cloned into the *Xho*I-*Mfe*I sites of pCMMP IRES GFP, generating pCMMP f-HEXIM1 and pCMMP HEXIM1-f [13]. The cytomegalovirus (CMV) promoter-driven *gag-pol* expression vector psyn*gag-pol* has been previously described by Wagner *et al.* [14] and pLTR*gag-pol* was constructed by cloning the *Mlu*I-*Hin*dIII fragment encoding the LTR from pNL-luc [15] into the *Mlu*I-*Hin*dIII sites of psyn*gag-pol*. The tax expressing plasmid pCGtax and pHTLV LTR luciferase were kindly provided by Dr. Watanabe (Tokyo Medical Institute). The *tat*-expressing plasmid pSVtat was a generous gift from Dr. Freed (National Cancer Institute-Frederick, Frederick, Maryland, USA). The plasmid pLTR-luc has been described previously (Miyauchi *et al.*, *Antiviral Chemistry and Chemotherapy*, in press). The following plasmids have been described previously by Komano *et al.* [13]: pVSV-G, pMD*gag-pol*, pTM3Luci, phRL-CMV and pSIVmac239ΔnefLuc.

Cells and transfection

All the mammalian cells were maintained in RPMI 1640 (Sigma, St Louis, Missouri, USA) supplemented with 10% fetal bovine serum (Japan Bioserum, Tokyo, Japan), penicillin and streptomycin (Invitrogen, Tokyo, Japan). Cells were incubated at 37°C in a humidified 5% CO_2 atmosphere. Cells were transfected using Lipofectamine 2000 according to the manufacturer's protocol (Invitrogen).

Western blotting

Cells were lysed with sample buffer, sonicated, and boiled for 5 min. Samples were separated on 8% sodium dodecyl sulfate-polyacrylamide gel electrophoresis gels and transferred to polyvinylidene difluoride membranes (Millipore, Billerica, Massachusetts, USA) for western blotting according to standard techniques. Membranes were blocked with Tris-buffered saline containing 0.05% Tween-20 (TBS-T) containing 5% (w/v) non-fat skim milk (Yuki-Jirushi, Tokyo, Japan) for 1 h at room temperature and incubated with primary antibodies including the M2 anti-FLAG epitope monoclonal antibody (Sigma), an anti-actin monoclonal antibody (MAB1501R; Chemicon/Millipore, Billerica, Massachusetts, USA), an anti-cyclin T1 rabbit polyclonal antibody (H-245; Santa Cruz Biotechnology, Santa Cruz, California, USA), an anti-cyclin T2a/b goat polyclonal antibody (A-20; Santa Cruz), an anti-p24 monoclonal antibody (183-H12-5C; NIH AIDS Research and Reference Reagent Program), an anti-HIS1 chicken polyclonal antibody (N-150; GenWay, San Diego, California, USA), and an anti-Bip/GRP78 monoclonal antibody (clone 40; BD Biosciences/Transduction Laboratories, San Jose, California, USA) for 1 h at room temperature. Membranes were washed with TBS-T and incubated with appropriate second antibodies including biotinylated anti-goat (GE Healthcare Bio-Sciences, Piscataway, New Jersey, USA) or anti-chicken IgY (Promega, Madison, Wisconsin, USA), and EnVision+ (Dako, Glostrup, Denmark) for 1 h at room temperature. For a tertiary probe, we used horseradish peroxidase (HRP)-streptavidine (GE Healthcare) if necessary. Signals were visualized with an LAS3000 imager (Fujifilm, Tokyo, Japan) after treating the membranes with the Lumi-Light Western Blotting Substrate (Roche Diagnostics GmbH, Mannheim, Germany).

Reporter assay

Luciferase activity was measured 48 h after transfection or infection using a DualGlo assay kit (Promega) according to the manufacturer's protocol. The beta-galactosidase activity was measured using a LumiGal assay kit (BD Biosciences/Clontech, San Jose, California, USA) according to the manufacturer's protocol. The

chemiluminescence was detected with a Veritas luminometer (Promega).

Monitoring viral replication

To monitor HIV-1 replication, the culture supernantants were subjected to either a reverse transcriptase assay [16] or an enzyme-linked immunosorbent assay (ELISA) to detect p24 antigens using a Retro TEK p24 antigen ELISA kit according to the manufacturer's protocol (Zepto Metrix, Buffalo, New York, USA). For simian immunodeficiency virus (SIV) a p27 antigen ELISA kit was used according to the manufacturer's protocol (Zepto Metrix). The signals were measured with a Multiskan Ex microplate photometer (ThermoLabsystems, Helsinki, Finland). For vaccinia virus, adenovirus, and herpes simplex virus (HSV)-1, the activity of reporter genes was measured as previously described [13].

Generating viruses

To produce HIV-1 and SIV, 293T cells were transfected with plasmids encoding proviral DNA of HIV-1 (pHXB2) or pSIVmac239ΔnefLuc and culture supernatants containing viruses were collected at 48 h post-transfection. Murine leukemia virus (MLV) and lentiviral vectors pseudotyped with VSV-G were produced as described previously by cotransfecting 293T cells with either the pNL-Luc and pVSV-G vectors or the pMD*gag-pol*, pVSV-G, and pCMMP vectors [13]. Green fluorescent cells were sorted by fluorescence activated cell sorter (FACS) Aria (Becton Dickinson, San Jose, California, USA).

Reverse transcriptase-polymerase chain reaction

Total RNA was isolated with an RNeasy kit (Qiagen GmbH, Hilden, Germany) according to the manufacturer's instruction. The reverse transcriptase (RT)-polymerase chain reaction (PCR) assay was performed with a One Step RNA PCR Kit (Takara, Otsu, Japan), imaged by a Typhoon scanner 9400 (GE Healthcare), and quantified with Image Quant software (GE Healthcare). For the amplification of endogenous HEXIM1, the forward primer 5′-ACCACACGGAGAGCCTGCAGAAC-3′ and the reverse primer 5′-TAGCTAAATTTACGAAACCAAAGCC-3′ were used. For the amplification of HEXIM1-f, the forward primer 5′-GTACCTGGAACTGGAGAAGTGCCC-3′ and the reverse primer 5′-CAATTGCTAGTCGTCATCGTCTTTGTAGTC-3′ were used. For cyclophilin A, the forward primer 5′-CACCGCCACCATGGTCAACCCCACCGTGTTCTTCGAC-3′ and the reverse primer 5′-CCCGGGCCTCGAGCTTTCGAGTTGTCCACAGTCAGCAATGG-3′ were used.

Quantitative real time polymerase chain reaction

The real time PCR reaction was performed in a DNA Engine Opticon 2 Continuous Fluorescence Detection System (Bio-Rad, Hercules, California, USA). The cellular genomic DNA and total RNA were extracted 48 h post-infection with a DNeasy kit (Qiagen) and RNeasy kit (Qiagen), respectively, according to the manufacturer's instruction. For the reagents, we used QuantiTect SYBR Green PCR and RT-PCR Kits (Qiagen). To estimate the amount of integrated HIV-1 DNA, Alu-LTR PCR was performed according to the method described previously using the following primers: for the first PCR, 5′-AACTAGGGAACCCACTGCTTAAG-3′ and 5′-TGCTGGGATTACAGGCGTGAG-3′, and for the second PCR, 5′-AACTAGGGAACCCACTGCTTAAG-3′ and 5′-CTGCTAGAGATTTTCCACACTGAC-3′ [17]. The beta-globin primers have been described previously [18]. To estimate the amount of HIV-1 RNA, the second PCR primers for the Alu-LTR PCR were used. The primers for cyclophilin A are described above.

Results and discussion

The HEXIM1 cDNA tagged with a FLAG epitope at either the amino terminus (f-HEXIM1) or the carboxy terminus (HEXIM1-f) was cloned in a mammalian expression plasmid (Fig. 1a). A luciferase assay revealed that the Tat-dependent enhancement of transcription from the HIV-1 LTR was reduced by co-transfecting HEXIM1-expressing plasmids, whereas neither Tat-independent basal transcription from the HIV-1 LTR nor CMV promoter-driven transcription was affected (Fig. 1b). An oncogenic retrovirus human T cell leukemia virus type 1 (HTLV-1) encodes for *tax*, a functional homologue of HIV-1's *tat*, that utilizes P-TEFb to enhance transcription from the LTR promoter [19]. However, *tax*-dependent enhancement of transcription was not affected by HEXIM1 in similar experimental conditions (Fig. 1c). To monitor the effect of HEXIM1 on HIV-1 replication, we introduced HEXIM1-expressing plasmids into HeLa-CD4 cells along with pNL4-3, which produces replication-competent HIV-1, and measured the RT activity in the culture supernatant 1 week post-transfection. Transfecting HEXIM1-expressing plasmids decreased the RT activity in a dose-dependent manner (Fig. 1d). Next, we asked whether the inhibition of viral replication was specific to HIV-1 by examining vaccinia virus, adenovirus, and HSV-1 replication. We found that the propagation of these three viruses was not inhibited by HEXIM1-f expression (Fig. 1e–g), suggesting that the inhibition of viral replication by HEXIM1 was HIV-1-specific.

To examine whether HEXIM1 negatively affects lentiviral replication in the physiologically relevant host, we isolated human T cell lines constitutively expressing HEXIM1-f. We cloned HEXIM1-f cDNA into a pCMMP (MLV retroviral vector plasmid (Fig. 2a). The plasmid encoded an internal ribosomal entry site (IRES)-mediated green fluorescent protein (GFP) expression cassette, so that MLV vector-infected cells

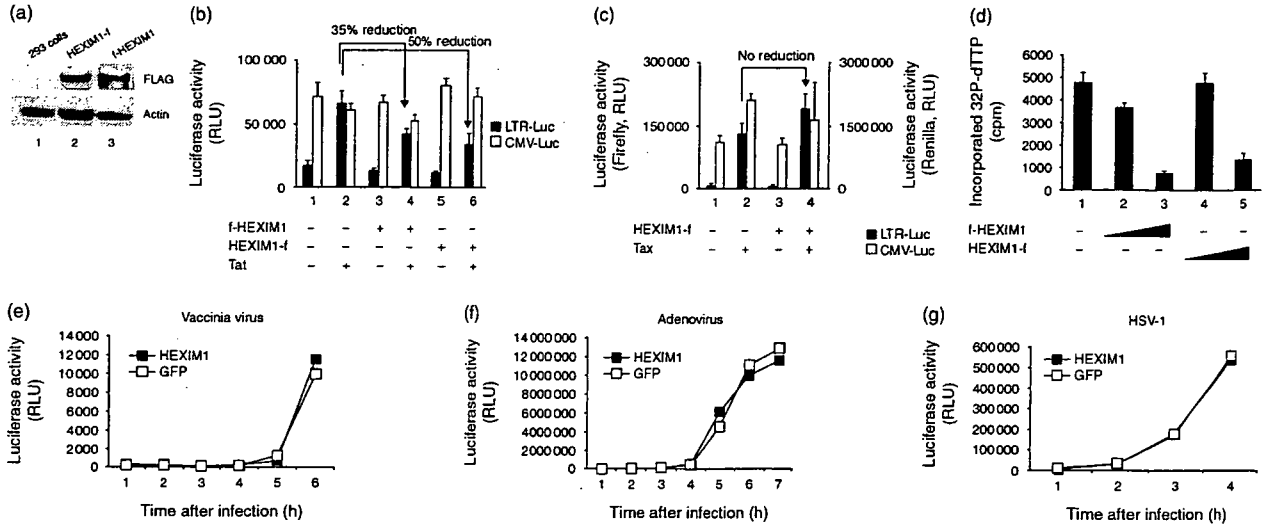

Fig. 1. Expression of hexamethylene bisacetamide-induced protein 1 (HEXIM1) specifically inhibits HIV-1 replication. (a) Detection of HEXIM1 cDNA tagged with a FLAG epitope at either the amino terminus (f-HEXIM1) or the carboxy terminus (HEXIM1-f) by western blot analysis in transiently transfected 293 cells (upper panel, approximately 65 kD). A western blot against actin is shown as a loading control (lower panel). (b) Expressing FLAG-tagged HEXIM1 decreased the luciferase activity driven by HIV-1 long terminal repeat (LTR) promoter in the presence of Tat (lanes 4 and 6, LTR-Luc, solid bars). However, FLAG-tagged HEXIM1 did not affect the expression of renilla luciferase from co-transfected plasmid driven by the cytomegalovirus (CMV) promoter (CMV-Luc, open bars). Representative data from three independent experiments done in triplicate are shown. Cells were transfected with 0.8 μg HEXIM1-expressing plasmid for the indicated lanes, 0.1 μg of pSV*tat* for the indicated lanes, and 0.1 μg of pLTR-Luc and 0.5 μg for phRL/CMV for all lanes. (c) Expressing FLAG-tagged HEXIM1 did not decrease the luciferase activity driven by HTLV-1 LTR promoter in the presence of Tax (lanes 2 and 4, LTR-Luc, solid bars) as well as renilla luciferase driven by the CMV promoter (CMV-Luc, open bars). Representative data from three independent experiments done in triplicate are shown. Cells were transfected with 0.8 μg of HEXIM1-expressing plasmid for the indicated lanes, 0.1 μg of pCGtax for the indicated lanes, and 0.1 μg of pHTLV LTR Luc and 0.5 μg for phRL/CMV for all lanes. (d) The dose-dependent reduction of HIV-1 production by transfection of HEXIM1-encoding plasmids (0.1 μg for lanes 2 and 4, 0.4 μg for lanes 3 and 5) along with a plasmid producing infectious HIV-1 (pNL4-3, 0.1 μg) in HeLa-CD4 cells. (e–g) Expressing HEXIM1-f did not limit the replication of vaccinia virus (e), adenovirus (f), or HSV-1 (g) in 293T cells. The *y*-axis represents the reporter gene activity, which reflects viral replication. Representative data from three independent experiments are shown. GFP, green fluorescent protein; RLU, relative light unit.

could be readily identified by the green fluorescence. Human T cell lines, including SUP-T1, MOLT-4, CEM, Jurkat, and M8166 were infected with MLV pseudotyped with vesicular stomatitis virus glycoprotein (VSV-G), and GFP-positive cells were collected with a FACS (Fig. 2a). For the negative control, we used MLV expressing GFP only. The successful introduction of HEXIM1-f into the cells was verified by RT-PCR and Western blot analysis (Fig. 2b and c). The total HEXIM1 protein expression in HEXIM1-f-transduced cells was approximately 3.7-, 1.5-, 2.0-, 4.8-, and 1.8-fold higher than in GFP-transduced cells in the CEM, Jurkat, MOLT-4, SUP-T1, and M8166 cell lines, respectively (Fig. 2c). To our surprise, the HEXIM1-f-expressing T cell lines remained GFP-positive, and therefore HEXIM1-f-positive, for more than 6 months and proliferated at rates almost indistinguishable from GFP-expressing cells. The expression levels of cyclin T1, cyclin T2, actin, and Bip/GRK78 in HEXIM1-f-expressing cells were almost identical to those in GFP-expressing cells, suggesting that the gene expression did not compensate the upregulated HEXIM1 (Fig. 2b and c). Expression of cyclin T2 was undetectable in M8166 cells (Fig. 2c). Similarly, HEXIM1-f expression did not affect the cell surface levels of the HIV-1 receptors CD4 and CXCR4 as demonstrated by FACS analysis (data not shown). These data indicate that the expression of HEXIM1-f did not reach levels where the physiological regulation of P-TEFb blocked cellular gene transcription.

The replication kinetics of HIV-1 or SIV was monitored by measuring the accumulation of viral capsid antigen in the culture medium. Strikingly, HIV-1 replicated more slowly in cells of all four T cell lines expressing HEXIM1-f than in cells expressing GFP (Fig. 2d–g). Similarly, HEXIM1-f-expressing M8166 cells supported SIV replication less efficiently than did GFP-expressing M8166 cells (Fig. 2h). Interestingly, the magnitude of HIV-1 replication delay was the most substantial in SUP-T1 cells, in which the levels of endogenous HEXIM1 were the lowest among the four cell lines tested for HIV-1 replication (Fig. 2c). Similar observations were made when the HIV-1 infection experiments were repeated, indicating that the expression of functional HEXIM1-f did not change over the course of the replication monitoring. We tested whether the viruses emerged in

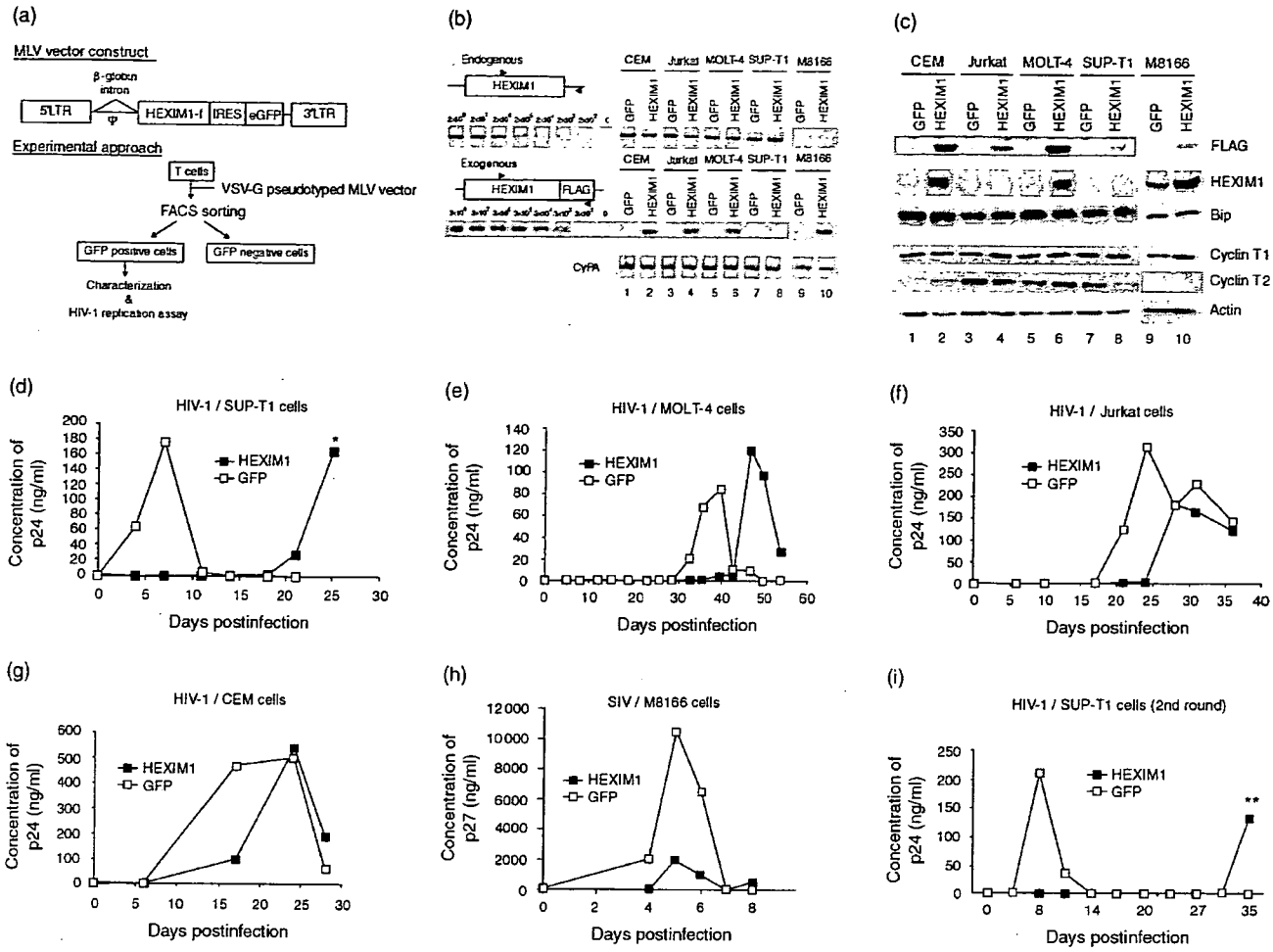

Fig. 2. Lentiviral replication is inhibited in various T cell lines constitutively expressing hexamethylene bisacetamide-induced protein 1 (HEXIM-1) cDNA tagged with a FLAG epitope at the carboxy terminus (HEXIM1-f). (a) The genomic organization of the retroviral vector expressing HEXIM1-f and a schematic representation of the experimental approach. (b) Detection of endogenous HEXIM1 and murine leukemia virus (MLV)-transduced HEXIM1-f (exogenous) mRNA by reverse transcriptase-polymerase chain reaction in green fluorescent protein (GFP)- and HEXIM1-f-expressing cells. The primer design is drawn schematically. Amplification efficiency was examined by using a known number of templates as standards for HEXIM1. Cyclophilin A (CyPA) was amplified to ensure the quality of the RNA. (c) Western blot analysis demonstrating expression of HEXIM1-f (denoted FLAG), endogenous HEXIM1 (HEXIM1), Bip, cyclin T1, cyclin T2, and actin in isolated T cell lines. (d–g) Replication profiles of HIV-1 (HXB2) in SUP-T1 (d), MOLT-4 (e), Jurkat (f), and CEM (g) cells either expressing HEXIM1-f or GFP alone. Representative data from two or three independent experiments are shown. (h) Replication profile of SIV in M8166 cells either expressing HEXIM1-f or GFP alone. Representative data from two independent experiments are shown. (i) The replication profiles of HIV-1 recovered from SUP-T1/HEXIM1-f cells (asterisk in Fig. 2d) in fresh SUP-T1/GFP or SUP-T1/HEXIM1-f. LTR, long terminal repeat.

HEXIM1-f-expressing cells were 'revertants' that might be able to replicate in HEXIM1-f-expressing cells as fast as in GFP-expressing cells. To address this, we recovered virus-containing culture supernatants from SUP-T1/HEXIM1-f cells at the peak of replication kinetics (asterisk, Fig. 2d). Then, both fresh SUP-T1/GFP and SUP-T1/HEXIM1-f were infected with the recovered virus and the replication kinetics was monitored. However, HIV-1 still replicated in SUP-T1/HEXIM1-f cells more slowly than in SUP-T1/GFP cells (Fig. 2i), akin to the original profiles (Fig. 2d), and the nucleotide sequences of LTR and *tat*, the primary targets of HEXIM1, remained unchanged (double asterisk in Fig. 2i). In addition, no mutations were found in viruses propagated in GFP-expressing SUP-T1 cells. Similar observations were made in MOLT-4 cells (data not shown). These data provide direct evidence that the expression of HEXIM1 inhibits lentiviral replication in human T cell lines.

Based on our experimental observations as well as the reported functions of HEXIM1, we assumed that the ability of HEXIM1 to limit HIV-1 replication was mostly due to the inhibition of Tat/P-TEFb-dependent transcriptional elongation. However, it was possible that HEXIM1 might also have targeted other viral replication

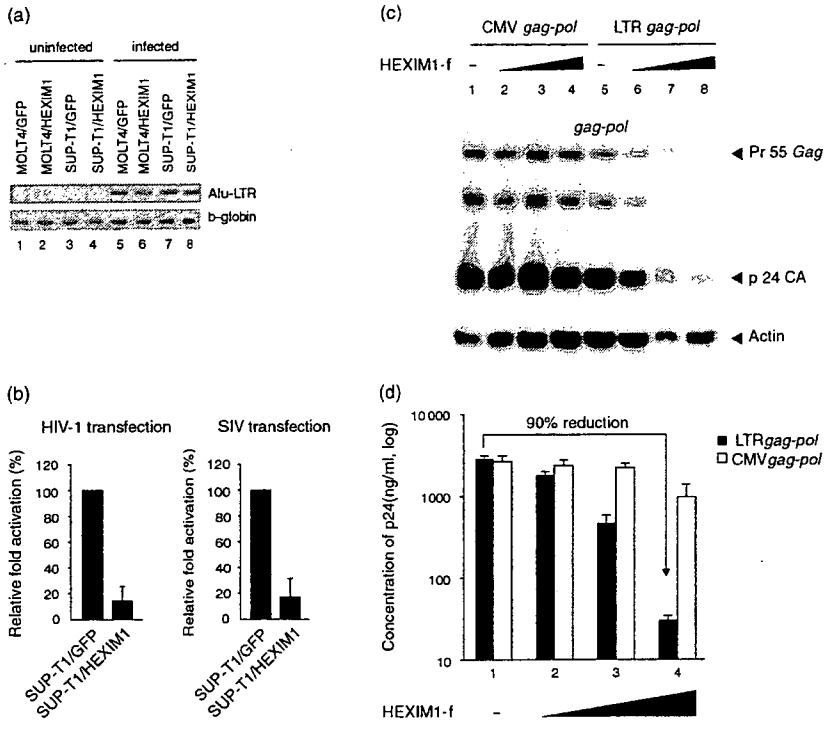

Fig. 3. Hexamethylene bisacetamide-induced protein 1 (HEXIM1) cDNA tagged with a FLAG epitope at the carboxy terminus (HEXIM1-f) does not affect the efficiency of viral integration or post-translational processes. (a) The Alu-long terminal repeat (LTR) and beta-globin polymerase chain reaction products from VSV-G-pseudotyped HIV-1-infected MOLT-4 and SUP-T1 cells expressing either green fluorescent protein (GFP) or HEXIM1-f alone were separated in an agarose gel and photographed. (b) The luciferase activities in SUP-T1/GFP or SUP-T1/HEXIM1-f cells electroporated with 10 μg of a plasmid encoding LTR-driven firefly luciferase plus 1 μg of phRL/cytomegalovirus (CMV). The firefly luciferase activity normalized to renilla luciferase activity in SUP-T1/GFP cells was set to 100%. The error bars represent the standard deviation of three independent experiments. (c) Western blot analysis showing Gag and its cleaved products expressed from either CMV promoter- or LTR promoter-driven *gag-pol* expression plasmid in the presence of pSVtat (0.1 μg, all lanes) and increasing amounts of HEXIM1-f (0.2 μg for lanes 2 and 6, 0.6 μg for lanes 3 and 7, and 2.0 μg for lanes 4 and 8). (d) The amount of p24 produced in the culture supernatant from cells analyzed in Fig. 3c was measured by enzyme-linked immunosorbent assay. Representative data from three independent experiments done in triplicate are shown. SIV, simian immunodeficiency virus.

steps. To test this possibility, we examined the viral entry and production processes separately. The efficiency of viral entry was analyzed by measuring the efficiency of viral integration. SUP-T1/GFP or SUP-T1/HEXIM1-f cells were infected with a replication-incompetent HIV-1 vector pseudotyped with VSV-G that expresses luciferase upon successful infection. We conducted an Alu-LTR PCR assay to detect the integrated viral genome. PCR products were detected only from HIV-1-infected cells (Fig. 3a). The signal intensities of Alu-LTR PCR products from GFP- and HEXIM1-f-experssing cells were similar. To compare the efficiency of viral infection as well as transcription quantitatively, we employed a real time PCR technique. Some infected cells were collected for an Alu-LTR PCR assay to quantify the amount of integrated viral genome, and the rest were processed to measure the amount of viral transcript as well as the luciferase activity. The amount of Alu-LTR PCR product from SUP-T1/HEXIM1-f cells was 3.5- and 3.3-fold more to that from SUP-T1/GFP cells from two independent experiments, respectively (Table 1). These data suggest that the efficiency of viral integration was not inhibited in HEXIM1-f-expressing SUP-T1 cells. In contrast, the relative abundance of HIV-1 transcript expressed in SUP-T1/HEXIM1-f cells was substantially decreased to 0.03 and 2.9% relative to SUPT1/GFP cells (Table 1). Furthermore, the luciferase activities were 200-fold lower in SUP-T1/HEXIM1-f cells than in SUP-T1/GFP cells (Table 1). Similar data was obtained from MOLT-4 cells infected with HIV-1 pseudotyped with VSV-G (data not shown). The transfection of plasmids encoding reporter viral DNA can bypass the viral entry and make it possible to measure the effect of HEXIM1 on LTR-driven transcription and translation. Consistent with above data, transfecting pNL-Luc into SUP-T1/HEXIM1-f cells gave significantly lower luciferase activities than SUP-T1/GFP cells (Fig. 3b, left). Similar data were obtained using pSIVmac239ΔnefLuc (Fig. 3b, right). These data strengthen the possibility that HEXIM1 targets post-integration processes.

Table 1. Effect of hexamethylene bisacetamide-induced protein 1 (HEXIM1) cDNA tagged with a FLAG epitope at the carboxy terminus (HEXIM1-f) on viral entry and transcription in SUP-T1 cells examined by quantitative real time polymerase chain reaction.

		Integrated HIV-1 genome			HIV-1 transcript			Luciferase activity	
Exp.	Transduced gene	Alu-LTR (copy)	β-globin (copy)	Normalized[a] (%)	HIV-1 RNA (copy)	CyPA (copy)	Normalized[b] (%)	RLU[c]	Normalized[d] (%)
1	GFP	5.2×10^5	6.7×10^6	100.0	1.6×10^6	6.8×10^7	100.0	3.2×10^5	100.0
	HEXIM1-f	2.0×10^6	7.4×10^6	351.3	6.7×10^1	1.0×10^8	0.03	1.5×10^3	0.5
2	GFP	4.6×10^6	1.8×10^7	100.0	3.1×10^8	8.9×10^7	100.0	7.1×10^5	100.0
	HEXIM1-f	1.6×10^7	1.9×10^7	333.2	9.4×10^6	9.3×10^7	2.9	3.4×10^3	0.5

[a]The number of Alu-long terminal repeat (LTR) products divided by the number of beta-globin products in SUP-T1/GFP is set to 100%. The abundance of Alu-LTR products in SUP-T1/HEXIM1-f relative to SUP-T1/green fluorescent protein (GFP) is shown.
[b]The number of HIV-1 RNA transcripts in SUP-T1/GFP divided by the number of cyclophilin A (CyPA) transcripts is set to 100%. The abundance of HIV-1 RNA in SUP-T1/HEXIM1-f relative to SUP-T1/GFP is shown.
[c]The luciferase activity is shown by relative light unit (RLU).
[d]The luciferase activity in SUP-T1/GFP is set to 100%. The luciferase activity in SUP-T1/HEXIM1-f relative to SUP-T1/GFP is shown.

To test this further, we analyzed the efficiency of post-transcriptional processes with a transient transfection assay measuring the amount of Pr55 Gag, a viral gene product, and virus-like particles (VLPs) produced in the culture supernatants. For this purpose, we used the CMV promoter-driven *gag-pol* expression plasmid, because HEXIM1-f did not affect CMV-driven transcription (Fig. 1b). At the levels of HEXIM1-f where LTR-driven Tat-dependent transcription was drastically inhibited (Fig. 3c, lanes 7, 8), the amount of CMV promoter-driven Gag expression was almost identical to that in the absence of HEXIM1-f (Fig. 3c, lanes 1–4). Furthermore, the processing pattern of Pr55 Gag in the presence of HEXIM1-f was identical to that in its absence (Fig. 3c). These data indicate that HEXIM1-f did not inhibit the transcription from a Tat-independent promoter, the translation of viral protein, or the protease activity of HIV-1. Finally, the potential effect of HEXIM1 on viral budding was examined. To do this, the amount of p24 CA in the culture supernatant of transfected cells was quantified as a representation of the amount of VLP. Expressing HEXIM1-f reduced VLP production from cells co-transfected with pLTR*gag-pol* and pSVtat at levels comparable to the protein expression levels (Fig. 3c and d). In contrast, expressing HEXIM1-f did not reduce the amount of VLP produced by cells co-transfected with pCMV*gag-pol* and pSVtat in conditions in which Tat-dependent LTR transcription was substantially inhibited (Fig. 3c and d). Taken together, this indicates that HEXIM1-f lowers the efficiency of Tat-dependent transcription from LTR promoter but does not block the efficiency of the late phase of the viral life cycle including translation, Gag's assembly, and budding. Thus, it is likely that HEXIM1 primarily targets Tat/P-TEFb-dependent transcription to inhibit HIV-1 replication.

Our findings demonstrated that HEXIM1, a cellular P-TEFb inhibitor, is a specific negative regulator of lentiviral replication in human T cell lines. The replication of vaccinia virus, adenovirus, and HSV-1 were not affected by HEXIM1-f expression; however, the *Tat*-dependent transcription of the LTR promoter of both HIV-1 and SIV was reduced by HEXIM1-f. HEXIM1 limited replication of HIV-1 dramatically at levels where it did not visibly affect cell physiology (as little as a 5-fold increase over the endogenous levels), nor were revertants immediately selected in HEXIM1-f-expressing cells. These data support the feasibility of developing HIV-1 inhibitors targeting the processes in which HEXIM1 is involved. For example, it is conceivable to hunt for a non-toxic chemical inducer for HEXIM1 since expression of HEXIM1 is induced by hexamethylene bisacetamide (HMBA) that is considerably toxic for cells [20].

P-TEFb has been shown to support transcription of the *c-myc* and CIITA transcription factors (reviewed in [21,22]). The functions of these transactivators are critical for cell proliferation, but in this study constitutive expression of HEXIM1-f, which reduces P-TEFb activity, did not affect the cell proliferation of human T cell lines, the human epithelial cell lines HEK293 or the NP2 glioblastoma cell lines (data not shown). How can this be explained? Very recently, a high-molecular-weight bromodomain protein, Brd4, was found to function as a 'cellular *tat*' [23,24]. Interestingly, it was shown that Brd4 binds not only to cyclin T1 but also to cyclin T2, a widely expressed variant of cyclin T, to which HEXIM1 binds but Tat does not [23–25]. We hypothesize that Brd4 might be able to recruit and activate P-TEFb more efficiently than does Tat, leaving cellular transcription unaffected by the upregulated expression of HEXIM1 from the retroviral vector. An alternative possibility comes from the fact that HEXIM1 does not interact with the ubiquitously expressed cyclin K, which functions as a P-TEFb component. It is possible that Tat is not able to utilize P-TEFb consisting of CDK9 and cyclin K but Brd4 can, such that cyclin K may substitute for cyclin T1 to support Brd4-mediated cellular gene transcription.

Acknowledgements

We thank Dr. Tsutomu Murakami for the critical reading of the manuscript. This work was partly supported by

Japan Health Science Foundation, Japanese Ministry of Health, Labor and Welfare, and Japanese Ministry of Education, Culture, Sports, Science and Technology.

Sponsorship: This work was partly supported by Japan Health Science Foundation, Japanese Ministry of Health, Labor and Welfare, and Japanese Ministry of Education, Culture, Sports, Science and Technology.

References

1. Marshall N, Price D. **Control of formation of two distinct classes of RNA polymerase II elongation complexes.** *Mol Cell Biol* 1992; **12**:2078–2090.
2. Kuiken C, Foley B, Hahn B, Korber B, Marx P, McCutchan F, *et al.*, editors. *HIV Sequence Compendium 2000.* Los Alamos: Theoretical Biology and Biophysics Group, Los Alamos National Laboratory, 2000.
3. Barboric M, Peterlin BM. **A new paradigm in eukaryotic biology: HIV Tat and the control of transcriptional elongation.** *PLoS Biol* 2005; **3**:e76.
4. Nguyen V, Kiss T, Michels A, Bensaude O. **7SK small nuclear RNA binds to and inhibits the activity of CDK9/cyclin T complexes.** *Nature* 2001; **414**:322–325.
5. Yang Z, Zhu Q, Luo K, Zhou Q. **The 7SK small nuclear RNA inhibits the CDK9/cyclin T1 kinase to control transcription.** *Nature* 2001; **414**:317–322.
6. Li Q, Price J, Byers S, Cheng D, Peng J, Price D. **Analysis of the large inactive P-TEFb complex indicates that it contains one 7SK molecule, a dimer of HEXIM1 or HEXIM2, and two P-TEFb molecules containing Cdk9 phosphorylated at threonine 186.** *J Biol Chem* 2005; **280**:28819–28826.
7. Michels A, Nguyen V, Fraldi A, Labas V, Edwards M, Bonnet F, *et al.* **MAQ1 and 7SK RNA interact with CDK9/cyclin T complexes in a transcription-dependent manner.** *Mol Cell Biol* 2003; **23**:4859–4869.
8. Yik J, Chen R, Pezda A, Samford C, Zhou Q. **A human immunodeficiency virus type 1 Tat-like arginine-rich RNA-binding domain is essential for HEXIM1 to inhibit RNA polymerase II transcription through 7SK snRNA-mediated inactivation of P-TEFb.** *Mol Cell Biol* 2004; **24**:5094–5105.
9. Barboric M, Kohoutek J, Price J, Blazek D, Price D, Peterlin B. **Interplay between 7SK snRNA and oppositely charged regions in HEXIM1 direct the inhibition of P-TEFb.** *EMBO J* 2005; **24**:4291–4303.
10. Schulte A, Czudnochowski N, Barboric M, Schonichen A, Blazek D, Peterlin B, Geyer M. **Identification of a cyclin T-binding domain in Hexim1 and biochemical analysis of its binding competition with HIV-1 Tat.** *J Biol Chem* 2005; **280**:24968–24977.
11. Fraldi A, Varrone F, Napolitano G, Michels A, Majello B, Bensaude O, Lania L. **Inhibition of Tat activity by the HEXIM1 protein.** *Retrovirology* 2005; **2**:42.
12. Michels A, Fraldi A, Li Q, Adamson T, Bonnet F, Nguyen V, *et al.* **Binding of the 7SK snRNA turns the HEXIM1 protein into a P-TEFb (CDK9/cyclin T) inhibitor.** *EMBO J* 2004; **23**:2608–2619.
13. Komano J, Miyauchi K, Matsuda Z, Yamamoto N. **Inhibiting the Arp2/3 complex limits infection of both intracellular mature vaccinia virus and primate lentiviruses.** *Mol Biol Cell* 2004; **15**:5197–5207.
14. Wagner R, Graf M, Bieler K, Wolf H, Grunwald T, Foley P, Uberla K. **Rev-independent expression of synthetic gag-pol genes of human immunodeficiency virus type 1 and simian immunodeficiency virus: implications for the safety of lentiviral vectors.** *Hum Gene Ther* 2000; **11**:2403–2413.
15. Masuda T, Planelles V, Krogstad P, Chen I. **Genetic analysis of human immunodeficiency virus type 1 integrase and the U3 att site: unusual phenotype of mutants in the zinc finger-like domain.** *J Virol* 1995; **69**:6687–6696.
16. Willey R, Smith D, Lasky L, Theodore T, Earl P, Moss B, *et al.* **In vitro mutagenesis identifies a region within the envelope gene of the human immunodeficiency virus that is critical for infectivity.** *J Virol* 1988; **62**:139–147.
17. Butler SL, Hansen MS, Bushman FD. **A quantitative assay for HIV DNA integration in vivo.** *Nat Med* 2001; 7:631–634.
18. Graf Einsiedel H, Taube T, Hartmann R, Wellmann S, Seifert G, Henze G, Seeger K. **Deletion analysis of p16(INKa) and p15(INKb) in relapsed childhood acute lymphoblastic leukemia.** *Blood* 2002; **99**:4629–4631.
19. Zhou M, Lu H, Park H, Wilson-Chiru J, Linton R, Brady JN. **Tax interacts with P-TEFb in a novel manner to stimulate human T-lymphotropic virus type 1 transcription.** *J Virol* 2006; **80**: 4781–4791.
20. Kusuhara M, Nagasaki K, Kimura K, Maass N, Manabe T, Ishikawa S, *et al.* **Cloning of hexamethylene-bis-acetamide-inducible transcript, HEXIM1, in human vascular smooth muscle cells.** *Biomed Res* 1999; **20**:273–279.
21. Price DH. **P-TEFb, a cyclin-dependent kinase controlling elongation by RNA polymerase II.** *Mol Cell Biol* 2000; **20**:2629–2634.
22. Garriga J, Grana X. **Cellular control of gene expression by T-type cyclin/CDK9 complexes.** *Gene* 2004; **337**:15–23.
23. Jang M, Mochizuki K, Zhou M, Jeong H, Brady J, Ozato K. **The bromodomain protein Brd4 is a positive regulatory component of P-TEFb and stimulates RNA polymerase II-dependent transcription.** *Mol Cell* 2005; **19**:523–534.
24. Yang Z, Yik J, Chen R, He N, Jang M, Ozato K, Zhou Q. **Recruitment of P-TEFb for stimulation of transcriptional elongation by the bromodomain protein Brd4.** *Mol Cell* 2005; **19**:535–545.
25. Napolitano G, Licciardo P, Gallo P, Majello B, Giordano A, Lania L. **The CDK9-associated cyclins T1 and T2 exert opposite effects on HIV-1 Tat activity.** *AIDS* 1999; **13**:1453–1459.

Hematopoietic stem cell–engrafted NOD/SCID/IL2Rγ^{null} mice develop human lymphoid systems and induce long-lasting HIV-1 infection with specific humoral immune responses

Satoru Watanabe,[1] Kazuo Terashima,[2] Shinrai Ohta,[3] Shigeo Horibata,[3] Misako Yajima,[4] Yoko Shiozawa,[1] M. Zahidunnabi Dewan,[2,3] Zhong Yu,[2] Mamoru Ito,[5] Tomohiro Morio,[6] Norio Shimizu,[1] Mitsuo Honda,[3] and Naoki Yamamoto[2,3]

[1]Department of Virology, Division of Medical Science, Medical Research Institute, Tokyo Medical and Dental University, Japan; [2]Department of Molecular Virology, Graduate School of Medicine, Tokyo Medical and Dental University, Japan; [3]AIDS Research Center, National Institute of Infectious Diseases, Tokyo, Japan; [4]Department of Infectious Diseases, National Research Institute for Child Health and Development, Tokyo, Japan; [5]Central Institute for Experimental Animals, Kanagawa, Japan; and [6]Department of Pediatrics and Developmental Biology, Graduate School of Medicine, Tokyo Medical and Dental University, Japan

Critical to the development of an effective HIV/AIDS model is the production of an animal model that reproduces long-lasting active replication of HIV-1 followed by elicitation of virus-specific immune responses. In this study, we constructed humanized nonobese diabetic/severe combined immunodeficiency (NOD/SCID)/interleukin-2 receptor γ-chain knockout (IL2Rγ^{null}) (hNOG) mice by transplanting human cord blood–derived hematopoietic stem cells that eventually developed into human B cells, T cells, and other monocytes/macrophages and dendritic cells associated with the generation of lymphoid follicle–like structures in lymphoid tissues. Expressions of CXCR4 and CCR5 antigens were recognized on CD4$^+$ cells in peripheral blood, the spleen, and bone marrow, while CCR5 was not detected on thymic CD4$^+$ T cells. The hNOG mice showed marked, long-lasting viremia after infection with both CCR5- and CXCR4-tropic HIV-1 isolates for more than the 40 days examined, with R5 virus–infected animals showing high levels of HIV-DNA copies in the spleen and bone marrow, and X4 virus–infected animals showing high levels of HIV-DNA copies in the thymus and spleen. Furthermore, we detected both anti–HIV-1 Env gp120– and Gag p24–specific antibodies in animals showing a high rate of viral infection. Thus, the hNOG mice mirror human systemic HIV infection by developing specific antibodies, suggesting that they may have potential as an HIV/AIDS animal model for the study of HIV pathogenesis and immune responses. (Blood. 2007; 109:212-218)

Introduction

Current animal models for either human immunodeficiency virus type 1 (HIV-1) or simian immunodeficiency virus (SIV) suffer from the lack of a system precisely mirroring human HIV infection and the progression to disease state.[1] In current animal models with HIV infection, such as chimpanzees, animals do not develop AIDS.[1] Past animal models for HIV infection have relied on humanized severe combined immunodeficiency (hSCID) mice models to study prospective anti-HIV drugs and vaccines. SCID-hu (Thy/Liv) mice, engrafted with human fetal thymus and liver tissue in the renal subcapsular region, were first reported as the small-animal model.[2] Because human T cells are generated within the engrafted thymus, this model has been used for the study of thymopoiesis[3-6] and hematopoiesis[7,8] under the burden of HIV-1 infection. However, this model allows for a limited systemic HIV-1 infection, which is restricted mainly to the engrafted thymus. Another HIV mouse model, hu-PBL–SCID mice engrafted with human peripheral blood mononuclear cells (PBMCs),[9] has been actively used as a tool in developing antiretroviral therapy.[9-11] However, the infection persists for only a short time in association with rapid loss of CD4$^+$ T cells because there is no active hematopoiesis or thymopoiesis.[9,12,13] Furthermore, these mouse models fail to mirror certain key aspects of the human immune response, lacking normal lymphoid tissue and functional human antigen-presenting cells such as dendritic cells (DCs).[14] Thus, although these mouse models are valuable as animal models for HIV infection, the development of a mouse model more analogous to human HIV infection is needed if we are to better understand HIV pathogenesis and develop successful anti-HIV therapies and preventive vaccines.

To solve the difficult issue about the development of an ideal HIV mouse model, we initially selected a humanized nonobese diabetic (NOD)/SCID interleukin-2 receptor (IL-2R) γ-chain knockout (NOG) mouse[15] as a model animal because it has been suggested that multilineage cells, including human T, B, and natural killer (NK) cells, differentiate in these mice when given transplants of human CD34$^+$ hematopoietic stem cells.[16-18] In the current study, we further reveal the kinetics of differentiation of human B and T cells, monocytes/macrophages, and DCs in the mice that received transplants, and we characterize the animals by infection with both CCR5 (R5)– and CXCR4 (X4)-tropic HIV strains. Since our hNOG mice show stable and systemic infection of both R5- and X4-tropic HIV for more than

Submitted April 20, 2006; accepted August 12, 2006. Prepublished online as *Blood* First Edition Paper, September 5, 2006; DOI 10.1182/blood-2006-04-017681.

The publication costs of this article were defrayed in part by page charge payment. Therefore, and solely to indicate this fact, this article is hereby marked "advertisement" in accordance with 18 USC section 1734.

the 40 days studied, and HIV-specific antibodies are detectable in the animals with high plasma viral loads and HIV-DNA copy numbers, we also discuss the suitability of HIV-hNOG mice as an animal model for HIV-1 infection.

Materials and methods

Transplantation of human CB-derived hematopoietic stem cells in NOG mice

Human cord blood (CB) was obtained from Saiseikai Central hospital (Minato-ku, Tokyo, Japan) and Tokyo Cord Blood Bank (Katsushika-ku, Tokyo, Japan) after obtaining informed consent. All research on human subjects was approved by the Institutional Review Board of each institution participating in the project. CB mononuclear cells were separated by Ficoll-Hypaque density gradient. $CD34^+$ hematopoietic stem cells were isolated using a magnetic-activated cell sorting (MACS) Direct CD34 Progenitor Cell Isolation Kit (Miltenyi Biotec, Bergisch Gladbach, Germany) according to the manufacturer's instructions. More than 95% of $CD34^+$ cells were positively selected after 2 time-enrichment manipulations. Cells were either immediately used for the transplantation or frozen until use. NOG mice were obtained from the Central Institute for Experimental Animals (Kawasaki, Japan) and maintained under specific pathogen–free (SPF) conditions in the animal facility of the National Institute of Infectious Diseases (NIID; Tokyo, Japan). Mice used in these studies were free of known pathogenic viruses, herpes viruses, bacteria, and parasites. They were housed in accordance with the Guidelines for Animal Experimentation of the Japanese Association for Laboratory Animal Science (1987) under the Japanese Law Concerning the Protection and Management of Animals, and were maintained in accordance with the guidelines set forth by the Institutional Animal Care and Use Committee of NIID, Japan. Once approved by the Institutional Committee for Biosafety Level 3 experiments, these studies were conducted at the Animal Center, NIID, Japan, in accordance with the requirements specifically stated in the laboratory biosafety manual of the World Health Organization. Female mice (6 to 10 weeks old) were irradiated (300 cGy) and 1×10^4 to 1.2×10^5 $CD34^+$ cells were intravenously injected within 12 hours.

Flow cytometry

The purity of CB-derived $CD34^+$ cells after separation was evaluated by double staining with FITC-conjugated anti–human CD45 (J.33) and PE-conjugated anti–human CD34 (Class III 581) (all from Beckman Coulter, Fullerton, CA). After transplantation (1-7 months), peripheral blood, spleens, bone marrow (BM), and thymi were collected for flow cytometric analysis following staining with the following monoclonal antibodies (mAbs): FITC-conjugated anti–human CD45 (J.33), CD3 (UCHT1), CD4 (13B8.2), CD19 (J4.119), CD45RO (UCHL1) (all from Beckman Coulter), and CCR5 (2D7; BD Pharmingen, San Diego, CA); PE-conjugated anti–human CD4 (13B8.2), CD8 (B9.11), CD19 (J4.119), CD45RA (ALB11) (all from Beckman Coulter), and CXCR4 (44717; R&D Systems, Minneapolis, MN); anti–mouse CD45 (YW62.3; Beckman Coulter); ECD-conjugated anti–human CD45 (J.33; Beckman Coulter); and PC5-conjugated anti–human CD8 (T8) and CD14 (Rm052) (all from Beckman Coulter). Flow cytometric analysis was conducted by 2- or 4-color staining using an EpicsXL (Beckman Coulter).

Immunohistochemistry

Organs were snap-frozen following embedding in OCT compound (Sakura Finetechnical, Tokyo, Japan). Frozen sections were air-dried and fixed in acetone. HIV-1–infected organs were fixed in 4% paraformaldehyde and embedded in OCT compound following immersion in gradient sucrose (5%-30%). Fixed samples were stained with the following mAbs: anti–human CD45 (1.22/4014; Nichirei, Tokyo, Japan), CD3 (UCHT1; DAKO, Glostrup, Denmark), CD20 (L26; DAKO), CD68 (KP1; DAKO), CD205 (MG38; eBioscience, San Diego, CA), and DRC-1 (R4/23; DAKO) for follicular dendritic cells (FDCs); anti–mouse FDC-M1 (BD Pharmingen) for murine FDCs; and HIV-1 Gag p24 (DAKO) for detection of infected cells. Biotin-labeled goat $F(ab')_2$ anti–mouse immunoglobulin (Ig; ICN Biomedicals, Aurora, OH)– or biotin-labeled mouse $F(ab')_2$ anti–rat IgG (Jackson ImmunoResearch Laboratories, West Grove, PA) was used as the secondary antibody. Samples were treated with alkaline phosphatase (AP) or horseradish peroxidase (HRP)–streptavidin conjugate (ZYMED Laboratories Inc, San Francisco, CA). BCIP/NBT, DAB, or AEC (all from DAKO) was used for the visualization. Photographs were taken by light microscopy (Leica DMRA; Leica Microsystems Wetzlar, Wetzlar, Germany) using Leica HC PLAN APO lenses (10×/0.40 NA PH1). Leica Q550 was used for image processing.

Measurement of human Igs in mice plasma

Plasma concentrations of human IgM, IgG, and IgA in NOG mice that received transplants of human stem cells were determined by conventional human Ig quantitation assay at BML Inc (Tokyo, Japan).

Cells and viruses

Human embryonic kidney 293T cells and monkey kidney COS7 cells were cultured in RPMI 1640 supplemented with 10% fetal bovine serum (FBS) and antibiotics. The 293T cells and COS7 cells were used for transfection of DNA plasmids containing HIV-1_{JRCSF} and simian/human immunodeficiency virus (SHIV)–C2/1, respectively. The SHIV-C2/1 strain contains the *env* gene of pathogenic HIV-1 strain 89.6.[19] Cell-free supernatant was collected and stored at −80°C before use. A primary clinical isolate, HIV-1_{MNp}, was kindly provided by Dr J. Sullivan of the University of Massachusetts Medical School (Worcester, MA). PBMCs isolated from HIV-1–seronegative individuals were cultured in RPMI 1640 supplemented with 10% FBS and antibiotics with 5 μg of phytohemagglutinin (PHA)/mL for 3 or 7 days (PHA-PBMCs). HIV-1_{MNp} was propagated in PHA-PBMCs, and cell-free virus stocks were stored at −80°C.

The 50% tissue-culture infectious dose ($TCID_{50}$) was determined using PHA-PBMCs and the endpoint dilution method. A 4-fold series of dilution was prepared from the virus stock, and then cells were mixed and cultured for 7 days for X4–HIV-1 and 14 days for R5–HIV-1 in RPMI 1640 supplemented with 20% FBS and antibiotics. The endpoints were determined by screening for the p24 antigen using Lumipulse (Fujirevio, Tokyo, Japan).

HIV-1 infection

All procedures for the infection and maintenance of NOG mice were performed in Biosafety Level 3 facilities at NIID under standard caging conditions. On days 102 to 132 after stem cell transplantation, 16 mice were inoculated intravenously with R5-tropic HIV-1_{JRCSF} (65 000 $TCID_{50}$) or X4-tropic SHIV-C2/1 (50 000 $TCID_{50}$). On days 18 to 43 after inoculation, plasma was collected to determine HIV-RNA copy numbers, and spleen cells were prepared as single-cell suspensions to analyze the CD4/CD8 ratio using flow cytometry. A number (14) of other mice were inoculated intravenously with R5-tropic HIV-1_{JRCSF} (200 or 65 000 $TCID_{50}$) or X4-tropic HIV-1_{MNp} (180 or 20 000 $TCID_{50}$) on days 126 to 146 after transplantation. On days 18 to 40 after inoculation, plasma was collected for the determination of HIV-RNA copy numbers, and single-cell suspensions of the spleen, BM, and thymus were prepared for HIV-DNA measurement. The CD4/CD8 ratio in the spleen and percentages of human $CD45^+$ cells in organs were analyzed using flow cytometry.

Virologic analysis

Plasma viral RNA copy numbers were measured using a real-time quantification assay based on the TaqMan system (Applied Biosystems, Foster City, CA). Plasma viral RNA was extracted and purified using a QIAamp Viral RNA Mini Kit (Qiagen, Valencia, CA). The RNA was subjected to reverse transcription (RT) and amplification using a TaqMan One-Step RT–polymerase chain reaction (PCR) Master Mix Reagents Kit (PE Biosystems, Foster City, CA) with HIV-1 gag consensus primers

(forward, 5′-GGACATCAAGCAGCCATGCAA-3′; and reverse, 5′-TGCTATGTCACTTCCCCTTGG-3′) and an HIV-1 gag consensus TaqMan probe (FAM-5′-ACCATCAATGAGGAAGCTGCAGAA-3′-TAMRA). For SHIV-C2/1 analysis, primers (forward, 5′-AATGCAGAGCCCCAAGAAGAC-3′; and reverse, 5′-GGACCAAGGCCTAAAAAACCC-3′) and a TaqMan probe (FAM-5′-ACCATGTTATGGCCAAATGCCCAGAC-3′-TAMRA) were designed for targeting the SIVmac239 gag region.[20] Probed products were quantitatively monitored by their fluorescence intensity with the ABI7300 Real-Time PCR system (PE Biosystems). To obtain control RNA for quantification, HIV-1 gag RNA and SIVmac239 gag RNA were synthesized using T7 RNA polymerase and pKS460. Viral DNA was extracted and purified using a QIAamp DNA Mini Kit (Qiagen). Determination of HIV-1 DNA copy numbers was performed by real-time PCR assay with TaqMan Master mixture (PE Biosystems). Primers (forward, 5′-GGCTAACTAGGGAACCCACTG-3′; and reverse, 5′-CTGCTAGAGATTTTCCACACT-3′) and probes (FAM-5′-TAGTGTGTGCCCGTCTGTTGTGTGAC-3′-TAMRA) were designed for targeting the HIV-1 long terminal repeat region, R/U5. The viral DNA was quantified using LightCycler (Roche Diagnostics, Almere, The Netherlands). Viral RNA and DNA were calculated based on the standard curve of control RNA and DNA. All assays were carried out in duplicate.

HIV-antigen ELISA

Levels of anti–HIV-1 Igs against recombinant HIV-1_{IIIB} Env gp120, recombinant HIV-1_{MN} Env gp120, and recombinant HIV-1_{IIIB} Gag p24 (all from ImmunoDiagnostics Inc, Woburn, MA) in plasma from HIV-1–infected and –uninfected control mice were determined using a standard enzyme-linked immunosorbent assay (ELISA). Microplates (96-well) were coated overnight with 200 ng/well antigens, and plasma diluted 1:20, 1:60, and 1:180 with PBS were incubated for 1 hour. AP-labeled anti–human Igs (γ, α, and μ; Sigma-Aldrich, St Louis, MO) were used as secondary antibodies. P-nitrophenylphosphate (pNPP) Solution (WAKO Chemical USA, Richmond, VA) was used for the visualization. The enzyme reaction was stopped by addition of 0.1 M NaOH and read at 405 nm. All assays were carried out in triplicate.

Statistical analysis

Data were expressed as the mean value ± standard deviation (SD). Significant differences between data groups were determined by 2-sample Student *t* test analysis. A P value less than .05 was considered significant.

Results

Reconstitution of human lymphoid systems in hNOG mice

The initial studies describing the construction of humanized SCID mice used the human PBMC for infection of immunodeficiency viruses.[9,12,21] However, these hu-PBL-SCID mice showed a partial infection to the R5 virus and a relatively limited period of viral replication. To construct a more suitable mouse model mimicking HIV-1 infection in humans, we selected human CB stem cells as a transplant for NOG mice. NOG mice were inoculated intravenously with human $CD34^+$ hematopoietic stem cells, and their development of human lymphoid systems were then monitored. After transplantation (2 months), human $CD45^+$ leukocytes were recognized in both PB and the spleen, but most of the cells were human B cells (Figure 1A). Human T cells began to be recognized clearly in PB and the spleen 4 months after transplantation (Figure 1B) and gradually increased in level, as did human B cells (Figure 1C).

In Figure 1D, we summarized percentages of human $CD3^+$ T cells in human $CD45^+$ cells from 38 mice from 39 to 213 days after transplantation. Human $CD3^+$ T cells clearly increased 100 days after transplantation in both PB and the spleen. After transplantation (4 months), human $CD3^+$ T cells in the spleen preferably expressed CD45RA rather than CD45RO (70.8% ± 13.4% and 27.3% ± 38.8% in $CD3^+$ T cells, respectively; n = 5; Figure 1E), demonstrating that most of the T cells were in a naive state. In addition, plasma taken from 5 mice 113 to 143 days after transplantation showed that all mice produced human IgM, with concentrations ranging from 0.025 to 0.5 g/L, and that human IgG and IgA was also detected in some of the mice (ranges, 0.015-0.18 g/L and 0.003-0.012 g/L, respectively) (data not shown).

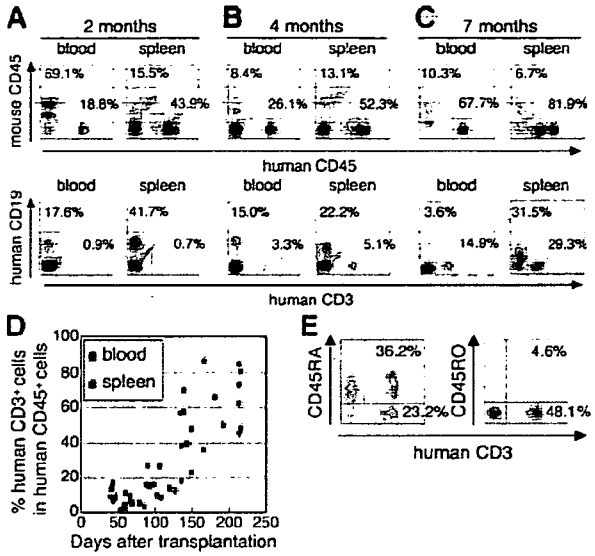

Figure 1. Flow cytometric analysis of human T cells in the peripheral blood and spleen in NOG mice given intravenous transplants of human CB-derived $CD34^+$ cells. (A-C) Representative profiles of the mice 2 months (A), 4 months (B), and 7 months (C) after transplantation. The ratio of human to murine $CD45^+$ cells and that of human $CD3^+$ to $CD19^+$ cells show an incremental increase in human $CD45^+$ cells and human $CD3^+$ cells from 2 to 7 months. (D) Change of net percentages of human $CD3^+$ T cells among human $CD45^+$ cells in peripheral blood and the spleen from 38 mice 39 to 213 days after transplantation. (E) CD45RA is more efficiently expressed than CD45RO on human $CD3^+$ T cells in spleen. A gate was set on the human $CD45^+$ population. The fluorescence-activated cell sorting (FACS) profile is representative of 1 in a group of 5 mice.

By 7 months after transplantation, human $CD45^+$ leukocytes comprised more than 80% to 90% of mononuclear cells in the spleen (Figure 1C), and most of the mice showed symptoms of a wasting condition and a hunched back. Based upon these results, we determined that the suitable period for HIV inoculation would be 4 to 5 months after transplantation.

Formation of lymphoid structures, including monocytes/macrophages, DCs, and FDCs

Next, using the hNOG mice at 4 months after transplantation, we investigated lymphoid structure formation and the development of human monocytes, macrophages, DCs, and FDCs, which are very important factors not only for elicitation of immune responses against foreign antigens, but also for the spread of HIV-1 infection in a body.[22-24] Human $CD14^+$ monocytes were detected in PB, the spleen, and BM using flow cytometry (Figure 2A). During immunohistochemical analysis, human $CD45^+$ leukocytes gathered in a form of follicle-like structures (FLSs) at the end of the central artery in the spleen (Figure 2B). From a serial section of the same region (Figure 2B-G), these structures consisted mainly of human $CD20^+$ B cells (Figure 2C) admixed with a small number of human $CD3^+$ T cells (Figure 2D). Hardly any human FDCs positive for DRC-1 were detected (data not shown), whereas a

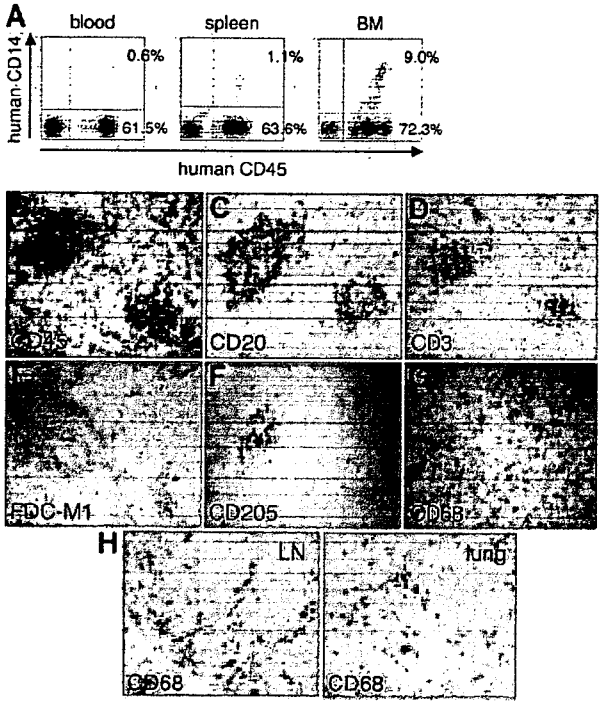

Figure 2. Flow cytometric analysis and immunohistochemical analysis of the expression of myelomonocytic markers in hNOG mice 4 months after transplantation. (A) Human CD14$^+$ monocytes/macrophages are recognized in peripheral blood, the spleen, and BM. (B-G) Immunohistochemical findings from serially sectioned spleen for the expressions of human CD45 (B), human CD20 (C), human CD3 (D), murine FDC (E), human CD205 (F), and human CD68 (G). (H) Human CD68$^+$ macrophages are also detected in the medulla of the LN and lung. Visualization was performed with BCIP (B-D, F-G), DAB (E), and AEC (H). Original magnification, ×100.

loose network of murine FDCs positive for FDC-M1 was recognized in the distal portion of the FLSs (Figure 2E). Human CD205$^+$ DCs were predominantly detected in a cluster form within the FLSs (Figure 2F), while human CD68$^+$ macrophages were scattered throughout the spleen (Figure 2G). Many human CD68$^+$ macrophages were also observed in various other organs, including the lymph nodes (LNs) and the lungs (Figure 2H).

Expression of HIV-1 coreceptors on CD4$^+$ cells in various tissues

Since the development of lymphoid tissues was recognized in hNOG mice, we focused on the expressions of HIV-1 coreceptors CXCR4 and CCR5 on human CD4$^+$ cells in these tissues. CXCR4 antigen was expressed in 36.5% ± 4.2% (n = 4) of the CD4$^+$ cells in PB (Figure 3A) and 78.1% ± 17.1% (n = 5) in the spleen (Figure 3B). CCR5$^+$ cells were detected in 15.5% ± 1.8% (n = 4) of CD4$^+$ cells in PB and 28.6% ± 12.6% (n = 5) in the spleen (Figure 3A-B). In the thymus, CD4$^+$CD8$^+$ thymocytes existed in 82.9% ± 4.4% (n = 5) as well as small numbers of CD4$^+$CD8$^-$ cells (6.4% ± 2.4%; n = 5) and CD4$^-$CD8$^+$ cells (7.7% ± 3.0%; n = 5), with the CXCR4 antigen expressed in 50.1% ± 4.5% (n = 5) of CD4$^+$ cells, while, as with normal human thymocytes,[25] CCR5$^+$ cells were almost undetectable, with less than 1% (0.6% ± 0.1%; n = 5) (Figure 3C). Human CD3$^+$ T cells and CD14$^+$ monocytes in BM were detected only in 3.2% ± 2.1% and 5.8% ± 3.8%, respectively, while CD4$^+$ cells were recognized in 18.1% ± 6.5%, with many expressing both CXCR4 (75.0% ± 23.1%) and CCR5 (81.3% ± 6.6%; n = 5; Figure 3D). Thus, distributions of HIV-1 coreceptor–positive cells in these lymphoid tissues suggest that the hNOG mice allow for sufficient development of human cells to make the study of HIV-1 pathogenesis possible.

Both R5- and X4-tropic HIVs efficiently infect and replicate in hNOG mice

In our preliminary study, using low and high doses of challenge virus, no viral infection was detected in any of the virus-inoculated hNOG mice at 7 days after infection, while some showed detectable plasma viral loads at 14 days (data not shown). Then, we prepared 16 hNOG mice that received transplants of stem cells and inoculated them with a high dose of R5-tropic HIV-1$_{JRCSF}$ (65 000 TCID$_{50}$) and X4-tropic SHIV-C2/1 (50 000 TCID$_{50}$) intravenously through the tail vein at 102 to 132 days after transplantation. Upon HIV-1$_{JRCSF}$ infection, viral copy numbers in plasma rose to a level of 1.6×10^5 to 5.8×10^5 copies/mL (n = 4) on day 33 and 2.0×10^5 to 4.7×10^5 copies/mL on day 43 (n = 4) (Figure 4A). Moreover, for SHIV-C2/1 infection, viral copy numbers in plasma were 1.6×10^3 to 3.2×10^5 copies/mL on day 18 (n = 4) and reached 5.4×10^4 to 1.1×10^5 copies/mL on day 42 (n = 4; Figure 4B). In these mice, no significant decline in the CD4/CD8 ratio was observed throughout entire period of follow-up for the R5-tropic virus infection, while CD4$^+$ cell decline was detected for the X4-tropic virus infection on day 42 after infection ($P = .044$) but not on day 18 after infection (Figure 4C). Four mice that did not receive transplants of human stem cells showed no detectable levels of plasma viral load (less than 500 copies/mL) following HIV/SHIV inoculation (data not shown).

To confirm HIV infection, we used immunohistochemistry to detect the presence of the p24 antigen of the HIV-1 Gag protein in various tissues of mice showing viremia. p24$^+$ cells were clearly identified in the spleen, LN, and lungs (Figure 4D), which include macrophage-like cells.

Different distributions of R5- and X4-tropic viruses in lymphoid tissues

A number of mice (14) were further analyzed for HIV-1 infection on days 126 to 146 after transplantation with a low dose (200 TCID$_{50}$) or a high dose (65 000 TCID$_{50}$) of R5-tropic HIV-1$_{JRCSF}$ and a low dose (180 TCID$_{50}$) or a high dose (20 000 TCID$_{50}$) of X4-tropic HIV-1$_{MNp}$. Consequently, 2 of the 4 mice given a low

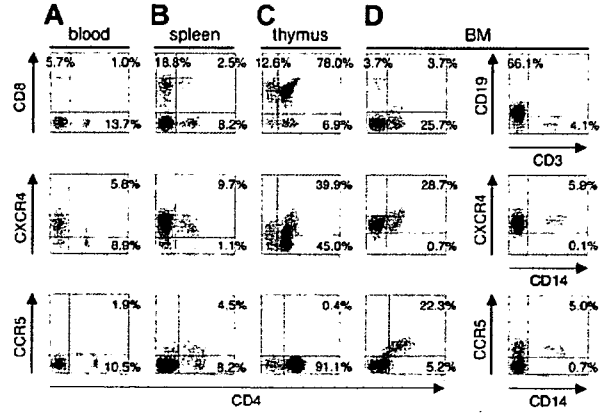

Figure 3. Surface expression of HIV-1 coreceptors on CD4$^+$ cells in various organs of mice 4 months after transplantation. A representative FACS profile of human CXCR4 and CCR5 on CD4$^+$ cells shows the existence of CXCR4$^+$CD4$^+$ and CCR5$^+$CD4$^+$ cells in blood (A), spleen (B), and BM (D), but no CCR5$^+$CD4$^+$ cells in the thymus (C). BM results show that many CD4$^+$ cells are neither CD3$^+$ T cells nor CD14$^+$ monocytes. A gate was set on the human CD45$^+$ population.

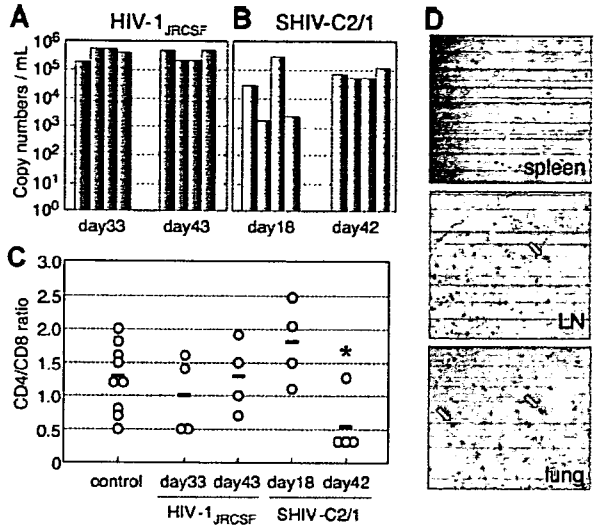

Figure 4. The numbers of RNA viral copies in plasma, CD4+/CD8+ T-cell ratios in the spleen, and p24 detection in the immunohistochemistry of HIV/SHIV-infected mice. (A) Viral copy numbers of 8 mice inoculated with a high infectious dose of HIV-1_{JRCSF} (65 000 $TCID_{50}$) and killed on days 33 and 43 after inoculation. (B) Viral copy numbers of 8 mice inoculated with a high infectious dose of SHIV-C2/1 (50 000 $TCID_{50}$) and killed on days 18 and 42 after inoculation. Note that all the mice showed high levels of viremia that lasted more than 40 days after inoculation. (C) CD4/CD8 cell ratios in the spleens of 16 infected mice and 9 uninfected control mice. Control mice were not inoculated with HIV/SHIV and were killed on days 105 to 166 after stem cell transplantation. There was no significant rapid loss of $CD4^+$ cells in HIV-1_{JRCSF}–infected mice, while a decline of the CD4/CD8 ratio was detected in SHIV-C2/1–infected mice on day 42 after infection compared with uninfected control mice ($^*P < .05$). The short bars indicate the means of each group. (D) $P24^+$ cells are clearly observed in the spleen, LNs, and lungs. Arrow indicates p24 positive for macrophage-like cells. Original magnification, ×100.

dose of HIV-1_{JRCSF} and 2 of the 3 mice given a low dose of HIV-1_{MNp} were successfully infected (Table 1), suggesting that each dose represents an approximately 50% infectious dose of HIV for hNOG mice. High HIV-DNA copy numbers were mainly detected in the spleen and BM of the HIV-1_{JRCSF} –infected mice, and in the thymus and spleen of the HIV-1_{MNp}–infected mice, while their BM showed lower copy numbers (Table 1).

Generation of HIV-specific antibodies in hNOG mice at a high multiplicity of infection

We then tested for generation of human antibodies against HIV-1 from these 14 mice by HIV antigen-specific ELISA. The sera of mice no. 136-3 and no. 157-3 infected with HIV-1_{JRCSF} and HIV-1_{MNp}, respectively, showed significant levels of human antibodies specific for HIV-1_{IIIB}-Env gp120 (Figure 5A), HIV-1_{MN}-Env gp120 (Figure 5B), and HIV-1_{IIIB}-Gag p24 (Figure 5C). In addition, no. 157-4 sera from an HIV-1_{MNp}–infected animal was also weakly positive for their Env and Gag antigens. These animals showed intense plasma viral loads and enhanced proviral DNA copies in the spleen, BM, and thymus (Table 1), suggesting that hNOG mice inoculated with high doses of HIV and showing high rates of viral infection develop HIV-1–specific humoral immune responses that are analogous to those seen in human anti-HIV B-cell responses.

Discussion

Current small-animal models fall short of accurately mirroring human HIV-1 infection and thus have limited usefulness in analyzing the natural course of its progression to the disease state and in developing antiviral countermeasures. Although successful HIV-1 infections in immunodeficiency mice humanized with PBMCs have been reported,[12,13,21] transplanted human cells are soon depleted and do not elicit virus-specific immune responses, shedding little light on pathogenesis and vaccine development. By using NOG mice that received hematopoietic stem cell transplants showing high rates of viral infection, we demonstrated HIV-specific antibody responses and viral infection parameters, including the following: (1) similar levels of susceptibility to both R5- and X4-tropic HIV-1; (2) high levels of viremia stably observed over 40 days; (3) immunohistochemical detection of infected cells in various organs; and (4) a distinct tissue distribution for R5- versus X4-tropic HIV-1s.

Among $CD4^+$ T cells, CXCR4 antigen is primarily expressed on naive and CCR5 on activated or memory cells.[26] hu-PBL-SCID mice become susceptible to R5-tropic HIV-1 strains,[27] since T cells

Table 1. Comparison of viral RNA copies in plasma and HIV-DNA copies in the spleen, BM, and thymus from hNOG mice receiving low- and high-dose viral inoculations

Mouse ID no.	HIV strain	$TCID_{50}$	Time after inoculation, d	RNA viral copies/mL	CD4/CD8 ratio	HIV-DNA copies/10^6 human cells		
						Spleen	BM	Thymus
Low-dose viral inoculation group								
113-1	HIV-1_{JRCSF}	200	18	6 240	1.8	34 177	11 785	3 495
112-2	HIV-1_{JRCSF}	200	18	<500	1.2	< 100	< 100	< 100
113-2	HIV-1_{JRCSF}	200	40	6 177	1.6	25 855	27 920	3 473
112-3	HIV-1_{JRCSF}	200	40	<500	0.9	< 100	< 100	<100
112-4	HIV-1_{MNp}	180	18	72 477	1.3	18 873	100	ND
113-4	HIV-1_{MNp}	180	40	70 667	0.3	4 947	653	32 163
112-1	HIV-1_{MNp}	180	40	<500	0.9	< 100	< 100	< 100
High-dose viral inoculation group								
136-3	HIV-1_{JRCSF}	65 000	25	252 381	0.8	958 871	1 797 600	232 155
136-2	HIV-1_{JRCSF}	65 000	29	50 167	0.7	41 172	54 521	8 600
141-1	HIV-1_{JRCSF}	65 000	30	67 667	2.2	27 735	52 430	429
161-3	HIV-1_{JRCSF}	65 000	30	13 847	0.9	104 466	14 653	111 080
157-3	HIV-1_{MNp}	20 000	31	1 253 925	0.5	41 053	56 802	976 556
157-4	HIV-1_{MNp}	20 000	31	147 973	0.6	3 634	262	40 796
161-6	HIV-1_{MNp}	20 000	31	108 073	1.7	4 991	< 100	3 673

Seven mice inoculated with a low infectious dose of HIV-1_{JRCSF} (200 $TCID_{50}$) or HIV-1_{MNp} (180 $TCID_{50}$), and 7 mice receiving a high infectious dose of HIV-1_{JRCSF} (65 000 $TCID_{50}$) or HIV-1_{MNp} (20 000 $TCID_{50}$) were listed.
ND indicates not done.